Global multinary structural chemistry of stable quasicrystals, high-T_C ferroelectrics, and high-T_c superconductors

K. M. Rabe
Department of Applied Physics, Yale University, New Haven, Connecticut 06520

J. C. Phillips
AT&T Bell Laboratories, Murray Hill, New Jersey 07974

P. Villars
Villars Intermetallic Phases Databank, Schwanden Postfach, 6354 Vitznau, Switzerland

I. D. Brown
Department of Physics, McMaster University, Hamilton, Ontario, Canada L8S 4M1
(Received 2 May 1991; revised manuscript received 1 November 1991)

A common feature of stable quasicrystals, high-T_C ferroelectrics, and high-T_c superconductors is that their unusual physical properties are correlated with characteristic crystal stuctures that are often vicinal to structural instabilities. We describe a statistically based diagrammatic scheme, due to Villars, for classifying the full database of crystal structures of binary, ternary, and quaternary compounds and tendency to compound formation in binary- and ternary-alloy systems. Principles of an expert system using this global organization to study small sets of compounds of special interest are formulated. Application to quasicrystals, ferroelectrics, and superconductors results in the identification of diagrammatic regularities which enable us to recognize phenomenological trends and to develop computerized search strategies for the prediction of new materials.

I. INTRODUCTION

The discovery of high-temperature superconductivity in pseudoperovskite cuprates has generated widespread interest in the crystal chemistry of complex materials. Not only high-temperature superconductivity, but also other intriguing properties, such as high-temperature ferroelectricity and stable quasicrystallinity, occur almost exclusively in systems containing three or more different elements. Clearly, the increased complexity creates opportunities which are just not present in the simpler binary systems. The challenge is to find systematic ways to identify trends in structure and stability of ternary systems, to understand why they are essential for the occurrence of these structural and electronic properties, and to predict the chemical compositions of new materials with these properties.

The aim of this paper is to make the regularities of crystal chemistry accessible to a wide audience by focusing on simple, yet remarkably accurate, descriptions of crystal structure and showing how these descriptions can clearly reveal deep relations between chemical composition, structure, and physical properties. The three properties we have chosen to study are quasicrystal formation, ferroelectricity, and superconductivity. At first sight it may seem that these three properties have nothing in common. However, if we restrict our attention to the ideal forms of these properties—*stable* quasicrystals, *high-T_C* ferroelectrics, and *high-T_c* superconductors—then we find that these always occur in *ternary,* not binary, compounds. Until recently very little was known about the global systematics of the structures even of binary compounds, and so it is not surprising that virtually nothing was known concerning the more complex case of ternary compounds. Our description of the global systematics of binary compounds can quite naturally be extended to ternaries, making it quite easy to compare binaries and ternaries and to relate characteristically ternary properties to structure and specific chemical composition. So far as we know, the present description is the only one which is capable of identifying and displaying these relations.

With these points in mind, we have organized this paper as follows. In Sec. II we discuss the background of our basic technique, quantum structural diagrams (QSD's). We describe the revolutions in scope and organization of the inorganic-compound database which have occurred in the last decade. It is this revolution which has made possible the emergence of our phenomenologically selected, but quantum-mechanically defined, QSD coordinates. These coordinates are dramatically superior to coordinates previously used by metallurgists, which seem superficially similar but which are in fact much less accurate, so much so as to contain little of statistical significance in structure-property correlations. The structural correlations are described for the simple case of binary compounds, where 3000 compounds have already been convincingly organized. This number far exceeds that previously organized for any group of inorganic materials. This point will necessarily be em-

phasized repeatedly, for not only is it the key to the success of any statistical approach, but also the absence of an adequate statistical basis in the past has often and deservedly earned a bad image for phenomenological chemical analyses based on the regularities of the Periodic Table.

Having determined the origin and values of the elemental coordinates by studying a large database composed of binary systems, we turn in Sec. III to the extension of this method to the structural analysis of ternary compounds. One important technical issue to be resolved is that of the correct generalization of the diagrammatic coordinate definitions. While there are certain obvious difficulties in generalizing the definition of difference coordinates, a few reasonable constraints produce a class of definitions which should be very similar in separating ability. A more fundamental issue is that of the relative incompleteness of the ternary database and the distribution of ternary systems among numerous structure types with only a few representatives each, making classification into individual structure types virtually impossible. This leads us to introduce the concept of "general structure type" defined by the types of coordination environments present in the structure. In fact, the organizing principle based on general structure types turns out to be so powerful that not only can we organize ternary compounds, but we will also be able to construct diagrams which combine binary, ternary, and quaternary compounds of arbitrary stoichiometric ratio. Significantly, this unification suggests that the general features of local structure in ternary systems do not crucially depend on the increase in complexity over binaries.

In Sec. IV we discuss the use of the diagrammatic approach for the separation of compound-nonforming from compound-forming intermetallic alloy systems. The distribution of the compound-nonforming regions in the "quantum formation diagrams" (QFD's) turns out to be completely different for binary and ternary systems (and, perhaps surprisingly, simpler for ternaries). As we shall see, this distinction reflects a fundamental difference in the determination of compound stability and marginal stability in binary and ternary systems. While it is clear that compound formation (or nonformation) is an even more fundamental property than structure, so far the QFD is the only successful characterization of this property for ternaries.

The remaining sections of this paper are devoted to the diagrammatic investigation of three types of physical properties: quasicrystallinity, high-T_C ferroelectricity, and high-T_c superconductivity. We will find, plotting compounds with these properties using the diagrammatic coordinates already determined, that they group into highly localized regions of the QSD and, in the case of quasicrystals, are also characterized by proximity to the compound-nonforming region of the QFD. It is important to note that the compounds with the same property group together, although they represent a variety of structure types; i.e., *the diagrammatic localization transcends crystal structure.* The application of diagrammatic conditions to the screening of candidate compositions thus can yield wide-ranging strategies for materials design.

In Sec. V we discuss the application of quantum diagrams to intermetallic ternary systems which form stable quasicrystals. Purely geometric sphere packing models of quasicrystal formation are unable to predict the occurrence of quasicrystallinity in real materials. In particular, they do not explain why there are no elemental or binary stable quasicrystals. Also, although stable quasicrystals are derived in these models from densely packed Frank-Kasper phases, of which there are about 400 examples, only a few stable quasicrystals are known. On the other hand, the localization of the quasicrystal forming systems in the QSD and QFD and the quantum diagram prediction of the stable Ga-Mg-Zn quasicrystal suggest that these diagrams correctly include the chemical content missing in these models. As we shall discuss in more detail, quasicrystal structures turn out to be energetically competitive with periodic structures only when the latter are nearly unstable.

In Sec. VI we use QSD's to study ferroelectricity. The connection between this phenomenon and lattice instabilities has long been known. Soft-mode models and scaling theories have provided a great deal of insight into the behavior of ferroelectrics near second-order (or nearly second-order) transitions. However, such models provide little understanding of how the chemistry of ferroelectric materials determines the transition temperature or the order of the transition. In contrast, the QSD technique focuses on precisely these nonuniversal, but experimentally important, features, which are also of great technological interest. As we shall see, it is particularly well suited to the identification of high-T_C ferroelectrics.

In Sec. VII we discuss the application of QSD's to high-temperature superconductivity. From a database of 70 compounds with $T_c > 10$ K and more than 20 different structure types, a diagram is constructed which shows a dramatic separation of high-T_c superconductors into three small islands *A*, *B*, and *C*. The copper oxide superconductors are all found in island *C* together with Chevrel sulfides and selenides. For superconductivity, the connections to lattice instabilities may seem less inevitable than for ferroelectricity, and a number of proposed mechanisms for high-T_c copper oxide superconductivity rely solely on nonlattice effects such as magnetic interactions or valence fluctuations. The diagrammatic analysis in fact reveals a strong association between high-T_C ferroelectrics and the high-T_c superconductors in island C. Our analysis vindicates a viewpoint long held by materials scientists, that long-range crystalline order is of secondary importance in explaining some of the chemical trends associated with high-T_C ferroelectric or high-T_c superconductive phase transitions.

The methods we describe in this paper are highly empirical and statistical in nature. It is not hard to recognize that such an approach can have enormous practical benefits. For example, one of us at one time labored long and unsuccessfully to synthesize a hypothetical binary *A* 15 compound, in the hope that it would be a high-T_c superconductor. With quantum diagrams it is easy to show, with a high degree of confidence, that this

hypothetical compound (and many others like it) probably does not exist. However, this inductive approach to the physics of crystals may at first seem opposed to, and even incompatible with, the deductive approach preferred by most physicists. In fact, the statistical approach complements the deductive one because the inductive approach can yield insights essential to the correct formation of a problem to be solved by more traditional deductive techniques. The ultimate concern of condensed-matter physics being the behavior of real materials, the most crucial and often the most difficult part of an analysis is the construction of an appropriate model. Unfortunately, many interesting phenomena occur in very complex materials for which simple chemical intuition and available calculational techniques are completely inadequate. In these cases, which include quasicrystallinity, high-T_C ferroelectricity, and high-T_c superconductivity, global diagrammatic analysis will prove invaluable in the identification of chemical trends, the construction of appropriate models, and the understanding of the origin of properties in the underlying crystal chemistry and structure, as well as in the theoretical prediction of these materials.

II. BINARY QUANTUM STRUCTURAL DIAGRAMS: DEVELOPMENT

It is a fundamental fact that the structure of a binary compound is determined by its composition. However, the justification of the occurrence of a particular structure for a given composition or, better yet, its prediction is a problem which has not yet been completely solved. Experience with a large number of compounds whose structures have been experimentally determined has led to the formation of the concepts of metallic, ionic, and covalent bonding and a body of guidelines for structural determination, collectively called "chemical intuition," based on analogies and extrapolations of observed correlations. The basic motivation of the development of diagrammatic techniques for global classification of crystal structures is to systematize and test "intuitive" ideas of chemical bonding in solids by putting them on a more quantitative and objective footing and, then, to extend them and make them more powerful.

In its most general form, the principle of the diagrammatic approach is to identify a few parameters, preferably functions of atomic properties of the constituents, which characterize the system and can be used simply and directly to determine its structure. From a first-principles point of view, we know that a complete characterization exists in terms of a very few parameters: the stoichiometry and atomic numbers of the constituent atoms. However, the dependence of the structure on these parameters is very ill behaved, with small changes in the values of the inputs generally leading to large changes in the resulting structure, and therefore is not well suited to an empirical analysis. A preliminary change of variables is required in which the stoichiometry and constituent atomic numbers are replaced by new parameters in a way designed to make the functional dependence of the structure optimally simple. Unfortunately, it is not feasible to derive the form of the new parameters directly from first principles. Indeed, the existence of such parameters is by no means guaranteed in a rigorous sense. The use of a small number of parameters (usually three or fewer), which imparts simplicity and clarity to the diagrams constructed with these coordinates, implies that this is a statistical and approximate, rather than fully deterministic, approach, which must be based on the analysis of large databases. Nevertheless, as we shall see, the procedures employed by the diagrammatic method are explicit and unambiguous. In this sense they represent a vastly preferable quantitative advance over fuzzy intuitive descriptions of chemical bonding in solids.

The pitfalls associated with the intuitive approach can easily be illustrated by example. It may seem obvious that empirical parameter scales, e.g., atomic size, developed for the analysis of structures of individual compounds ought to be useful in the diagrammatic method. In fact, it can be shown by counterexamples that just the opposite is true,[1] and it is necessary at the outset to distinguish between such scales, which we will refer to as "crystallographic coordinates" and "diagrammatic coordinates," which are specifically designed to classify many compounds with different structures and to separate them into disjoint groups. Later in this section, after we have described the nature of the best diagrammatic coordinates presently known, we will be able to explain this in detail. For the moment we point out that diagrammatic coordinates are designed to optimize separation only when all three scales are used in conjunction. With this condition the selection of diagrammatic coordinates is beyond the power of human intuition and must be performed through the statistical analysis of large databases.

The evolution of structural diagrams has been reviewed briefly in several recent articles,[1,2] and a more comprehensive review of the current situation will soon be available.[3] Here we remark that experience has shown that to make a single structural separation defining one diagrammatic coordinate, about 20–30 compounds are needed, to identify two coordinates, 60–100 compounds, and to determine three coordinates, 200–400 or more compounds are necessary. These numbers are very important because, as we shall see, three coordinates are necessary for the complete separation of binary compounds into structure types. It is the large magnitudes of these numbers that prevented most early efforts from being successful. This becomes clear in the context of the most successful early theories. Thus the metallurgical database up to about 1960 was organized by Pearson using two-coordinate diagrams containing between 10 and 60 compounds each.[4] The database was too sparse to lead to conclusive results, but it was clear that with a larger database some success might be achieved. The semiconductor database was organized by Phillips and Van Vechten.[5] By restricting themselves to $A^N B^{8-N}$ (non-transition-metal) octet compounds, of which there are about 80, they were successful in explaining not only structural trends, but also many structure-property relations using two coordinates (the covalent and ionic bond components). The success here, however, gave no indica-

tion of how the theory was to be extended to a wider range of compounds, including metals and insulators containing both transition and nontransition elements. Also with a two-coordinate scheme, more recently Zunger[6] has organized a much larger database of 565 AB compounds (including transition metals) into 34 structure types with an impressive success rate of 93%. However, it was necessary to construct separate diagrams for the octet and nonoctet cases and to permit regions assigned to different structure types to overlap. This made it clear that a three-coordinate scheme, which could only be constructed with the aid of an even larger database, would be necessary for complete structural separation.

During the last ten years the entire situation with regard to the statistical foundations of quantum structural diagrams has been altered in two basic respects. First, the database has been greatly enlarged. For inorganic compounds (excluding ternary oxides and halides), the number of compounds has been expanded from about 8000 to more than 22 000.[7] A different database, devoted to oxides and halides, includes about 10 000 compounds.[8] Second, recognition of the importance of structure type as a tool for compound classification is increasing. For ternary and quaternary oxides and halides, generally no structure type assignment has yet been made. However, in the case of the intermetallics, for all entries the structure type has now been assigned either by the author or the database editors.[7] Moreover, the intermetallic compounds have been listed by structure type as well as by composition. This listing is essential for success in constructing and interpreting structural diagrams.

With this massive expansion and much improved organization of the database, it finally became possible to identify the optimal diagrammatic coordinates for structural analysis using a manifestly statistical approach. The number and precise definitions of the coordinates are established not by heuristic arguments, but through the statistical analysis of the structural correlations of more than 3000 binary compounds. Only through such an approach can the accuracy of the diagrammatic method be pushed to its intrinsic limit. And, as we shall see, the optimal coordinate definitions do after all naturally lend themselves to physical interpretation.

The statistical analysis proceeds as follows.[9] First, 53 different atomic properties, which with various methods of determination produced 182 parameter scales, were analyzed to examine trends as a function of atomic number. The survey included 15 published data sets of ionic radii, 6 of metallic radii, 3 of covalent radii, 7 of the melting point, 6 of the heat of fusion, 13 of electronegativity, 5 of hardness, and so on. The parameter scales were divided into five different classes (labeled $A-E$) based on the directions of trends and locations of discontinuities in values or slope. For each class a typical parameter scale is chosen and a set of diagrammatic coordinates is constructed based on arithmetic combinations of the parameters. The relative efficacy of the resulting "candidate" coordinate definitions for the separation of structures or other desired properties is assessed by analyzing a "significant subset" of the database. The most successful definitions are then used to generate another set of candidate definitions by replacement of the atomic parameter scale with others in the same class. From this set the final choice of diagrammatic coordinates is made. This division of the optimization procedure into two steps is based on the idea that the separation efficiency is mainly determined by the type of trend, as described by the class, with smaller variations between parameter scale within each class which can be used in refining the coordinate definitions to yield diagrams of maximal quantitative usefulness.

In the case of binary structures, the significant subset was the 580 compound set with NaCl and CsCl structures. These are "Sammelbecken" structures which include compounds with all types of bonding and physical properties.[9] From the analysis of this significant subset, several conclusions emerged. The first was that three (and only three) coordinates are statistically necessary and sufficient. These were anticipated in previous work and are the valence-electron-number sum $\sum N_v$ and the size and electronegativity differences $|\Delta R|$ and $|\Delta X|$. However, from the comparison of the more than 20 atomic size scales and nearly 30 electronegativity scales (and related quantities), a second and quite gratifying conclusion was reached. In both cases the optimal parameter scales were substantially better than the others and had only relatively recently been formulated. The average-ionization-energy definition[10] of electronegativity was introduced in 1980. The pseudopotential definition of atomic core size,[1,2,11] which emerged in the 1970's, was in fact the single atomic parameter scale used by Zunger and Cohen[6] and previous quantum theorists[12] for the organization of crystal structures of binary compounds. Moreover, both these parameter scales are based on atomic energy levels and so are inherently quantum mechanical, as distinguished from almost all the other definitions, which are essentially empirical. The ability of the statistical analysis decisively to identify these more fundamental spectroscopic coordinates is a strong indication of the validity of the procedure, which was constructed to be as objective as possible. Furthermore, we shall see that the same coordinate definitions are equally successful for a variety of diagrammatic applications. Thus it seems that these quantum-mechanical atomic parameter scales are without doubt accurate indicators of the behavior of atoms in solids.

The three atomic parameter scales appearing in the QSD coordinate definitions—valence electron number, pseudopotential core radius, and spectroscopic electronegativity—are given in Fig. 1 for all 89 elements in the Periodic Table except the inert gases and the transuranic elements. The precise definitions and physical interpretations of these atomic parameter scales are discussed further in the Appendix. Here we comment only that the "chemical similarity" of two elements is determined by comparing the values of *all three* atomic parameters. An alternative approach to diagrammatic construction, involving the use of a single chemical similarity scale, has been successfully applied to binary compounds.[13]

We now discuss the applications of these coordinates to diagrammatic separations of binary compounds.[9]

H 1 2.10 1.25																
Li 1 0.90 1.61	Be 2 1.45 1.08											B 3 1.90 0.795	C 4 2.37 0.64	N 5 2.85 0.54	O 6 3.32 0.465	F 7 3.78 0.405
Na 1 0.89 2.65	Mg 2 1.31 2.03											Al 3 1.64 1.675	Si 4 1.98 1.42	P 5 2.32 1.24	S 6 2.65 1.10	Cl 7 2.98 1.01
K 1 0.80 3.69	Ca 2 1.17 3.00	Sc 3 1.50 2.75	Ti 4 1.86 2.58	V 5 2.22 2.43	Cr 6 2.00 2.44	Mn 7 2.04 2.22	Fe 8 1.67 2.11	Co 9 1.72 2.02	Ni 10 1.76 2.18	Cu 11 1.08 2.04	Zn 12 1.44 1.88	Ga 3 1.70 1.695	Ge 4 1.99 1.56	As 5 2.27 1.415	Se 6 2.54 1.285	Br 7 2.83 1.20
Rb 1 0.80 4.10	Sr 2 1.13 3.21	Y 3 1.41 2.94	Zr 4 1.70 2.825	Nb 5 2.03 2.76	Mo 6 1.94 2.72	Tc 7 2.18 2.65	Ru 8 1.97 2.605	Rh 9 1.99 2.52	Pd 10 2.08 2.45	Ag 11 1.07 2.375	Cd 12 1.40 2.215	In 3 1.63 2.05	Sn 4 1.88 1.88	Sb 5 2.14 1.765	Te 6 2.38 1.67	I 7 2.76 1.585
Cs 1 0.77 4.31	Ba 2 1.08 3.402	La 3 1.35 3.08	Hf 4 1.73 2.91	Ta 5 1.94 2.79	W 6 1.79 2.735	Re 7 2.06 2.68	Os 8 1.85 2.65	Ir 9 1.87 2.628	Pt 10 1.91 2.70	Au 11 1.19 2.66	Hg 12 1.49 2.41	Tl 3 1.69 2.235	Pb 4 1.92 2.09	Bi 5 2.14 1.997	Po 6 2.40 1.90	At 7 2.64 1.83
Fr 1 0.70 4.37	Ra 2 0.90 3.53	Ac 3 1.10 3.12														

Ce 3 1.1 4.50	Pr 3 1.1 4.48	Nd 3 1.2 3.99	Pm 3 1.15 3.99	Sm 3 1.2 4.14	Eu 3 1.15 3.94	Gd 3 1.1 3.91	Tb 3 1.2 3.89	Dy 3 1.15 3.67	Ho 3 1.2 3.65	Er 3 1.2 3.63	Tm 3 1.2 3.60	Yb 3 1.1 3.59	Lu 3 1.2 3.37
Th 3 1.3 4.98	Pa 3 1.5 4.96	U 3 1.7 4.72	Np 3 1.3 4.93	Pu 3 1.3 4.91	Am 3 1.3 4.89							

FIG. 1. Values of the atomic parameter scales used in the construction of the QSD (from Ref. 9). The first line in each box gives the element symbol and valence-electron number N_v, the second line gives the Matynov-Batsanov electronegativity X [in $(\text{eV})^{1/2}$], and the third line gives the pseudopotential core radii sum $R = r_s + r_p$ (in a.u.).

Somewhat more than 1100 AB compounds are known, and about 1000 of these are contained in 20 major structure types containing 5 or more compounds. Only one major structure type is excluded from this analysis—the NiAs type, which is a defect structure apparently stabilized by covalent directional relaxation energies near vacancies and has been discussed separately.[14] With the diagrammatic coordinates $\sum N_v$ and the magnitudes $|\Delta R|$ and $|\Delta X|$, the structural separation is 98% successful (22 violations among 1000 compounds). Overlapping regions are permitted only in cases where at least some of the compounds in the region show polymorphism. We show in Fig. 2 a cross section of the three-dimensional diagrammatic volume corresponding to $\sum N_v = 8$. This is the same as Fig. 3(f) of Ref. 9, except that we have distinguished compounds containing d- or f-transition-metal elements from those that contain only simple s-p metallic elements. The point is that the diagrammatic separation is unbiased and is equally successful for both kinds of compounds. By contrast, in first-principles calculations experience has shown that it is useful and desirable to treat the two types of compounds by different methods (partial waves for transition metals, pseudopotentials for simple metals). Of course, this balanced approach is possible only because the diagrammatic picture is much less detailed, but at the same time this means that the diagrammatic picture properly abstracts those general structural features which are independent of orbital content. No other method is known which does this.

After the initial success with simple binary AB compounds, structural diagrams were constructed for 1000 AB_2 compounds in 26 structure types (97% successful),[15] 650 AB_3 compounds in 21 structure types (98% successful),[16] and for 390 A_3B_5 compounds in 9 structure types (99% successful).[16] The coordinate definitions used were the same as for AB compounds except that the sign as

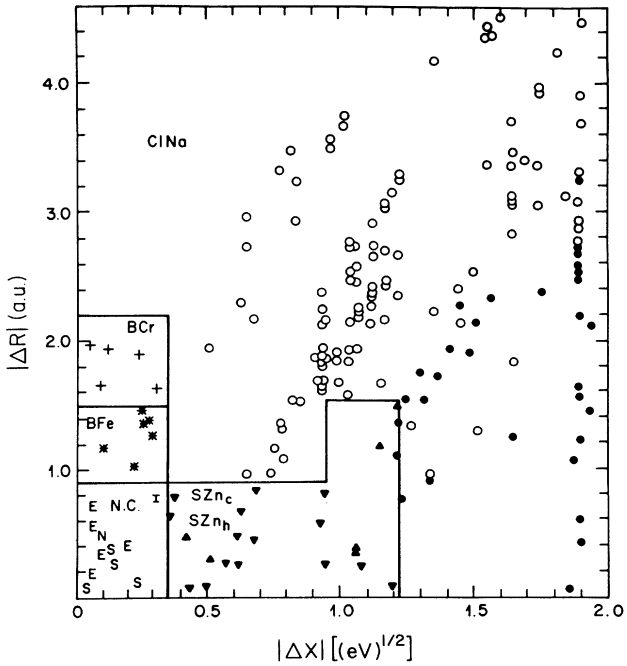

FIG. 2. Example of a binary quantum structural diagram for $A^N B^{8-N}$ compounds, taken from Ref. 9, but refined to distinguish between compounds which contain transition metals, rare earths, or actinides (crosses, stars, and open circles) and those which do not (solid symbols).

well as the magnitude of ΔR and ΔX was included, incorporating the structural distinctions between minority and majority elements. In fact, even in the equiatomic case, AB symmetry does not actually completely justify the use of magnitude only, since compounds for which ΔR and ΔX have the same sign are expected to be different from those in which they have different signs. However, the diagrammatic analysis shows that for AB compounds this distinction is relatively unimportant. Tests showed that including composition weighting in the coordinate definitions does not lead to significant improvements in separation. However, composition-dependent coordinates can be useful, for example, to include compounds of arbitrary stoichiometry on a single diagram in a more general structural classification scheme, to be discussed in Sec. III. In the present binary structure type classification, with a total of 4 diagrams (one for each stoichiometric ratio), altogether more than 3000 compounds in nearly 80 structure types are successfully separated with only 2.5% errors. In addition, for smaller sets of compounds with other binary stoichiometries 1:5, 1:12, 2:23, 2:17, and 2:3, the same coordinates have been used to construct diagrams which are approximately 99% successful.[17]

The remarkable success of the QSD technique in the global organization of the crystal structures of binary compounds is incontrovertible. However, the use of a statistical approach in the development of the scheme is not in itself helpful in elucidating the physical content and the reasons for the high accuracy of the QSD. Thus it is instructive to examine more closely a few general aspects of the diagrams.

One of the most important simplifying features of the QSD is that the diagrammatic coordinates are constructed from atomic parameter scales where exactly one parameter is assigned to an atom independent of crystal environment. Experience with crystallographic ionic, metallic, and covalent radii scales, which do depend on crystal environment, might cause concern that this transferability of parameters is impossible to achieve. In fact, as illustrated by the comparison[1] between cubic crystallographic radii and diagrammatic pseudopotential radii, the distinction between crystallographic and diagrammatic parameters lies precisely in the disentangling and separation in the latter case of the several factors—core radii, valence-electron number, and electronegativity—which combine to produce environment-dependent crystallographic parameters. Therefore, with the use of *three* carefully chosen coordinates, the required level of independence and transferability can be attained.

In the majority of cases, structural boundaries lie parallel to one or more coordinate axes. This implies that the energy balance which picks out one of the two adjacent structure types is essentially independent of this coordinate. This mutual independence of coordinates makes it possible in many cases to construct simple arguments identifying the factors favoring particular structure types and leads us to suppose that mutual independence is a key factor is producing a high level of structural separation.

The QSD technique, as described above, combines a pleasing naturalness with a success rate consistently over 95% in separating structures of A_nB_m compounds. The misplaced compounds may either reflect true inadequacies of the diagrammatic description or problems in the database, which can be expected to become apparent also at about this level of accuracy. These problems include various kinds of experimental uncertainty, particularly in structural determinations, uncertainties in concentration, impurity effects, and typographical errors. Thus further investigation of the remaining 5% must be conducted on a case-by-case basis.

One reason that a compound is misplaced on the diagram may be that its structure is stabilized by factors not included in the QSD description, which are usually of secondary importance. The most significant of these is the formation of *s-p* or *p-d* directional hybridized covalent bonds. In fact, as discussed further in the Appendix, a number of covalently stabilized structure types are correctly separated in the diagrams by virtue of strong localization along $\bar{N}_v$. The present database is too small to identify a fourth coordinate which might describe the more subtle structural effects of directional bonding. In particular, there is no appropriate "significant subset" with a sufficient number of compounds for statistical analysis. In addition, the definition of this coordinate would be complicated because it would necessarily have to include explicitly the difference between simple and transition metals. Finally, with a fourth coordinate much of the ease with which diagrams can be visualized would be lost. With the success rate already so high, these complications are too high a price to pay for a gain in accuracy of at most a few percent.

In fact, in absolute terms the number of exceptions is quite small. The investigation of the individual violations can prove to be highly informative. In a number of cases, this investigation has led to the correction of bibliographic errors or the identification of problems in experimental procedure.[18] Even more interesting is the investigation of "true" violations in order to identify the factors which anomalously dominate their structural chemistry. As mentioned above, these are often found to arise from directional bonding. Another noted exception, the NiAs structure, has been proposed to be stabilized by a large concentration of antisite defects.[14] Additional examples of interesting exceptions may be drawn from the compounds which have structural types with five or fewer representatives and thus were not included in the statistical analysis. While for many of these the paucity of representatives may be due to unusual restrictions on values of diagrammatic coordinates or simply a lack of experimental data, more often the stabilization of an uncommon structure type may be produced by exceptional factors.

Another consequence of the relatively small number of violations is that a number of useful applications of the QSD classification are possible. The energy cost for transforming a compound lying near a structural boundary into a hypothetical form with the adjacent structure type is likely to be quite small. In fact, this transformation may in some cases actually occur as a function of

pressure or temperature. This method of identifying systems with structural phase transitions has recently proved successful in an investigation of $ThAl_2$.[19] For the same reason, comparison with the energies of adjacent structure types can be used to provide the strictest test of a first-principles calculation of the structure of a particular compound. For example, AsCr, experimentally observed to have the MnP structure, could be studied in the NaCl, CW, FeSi, and CsCl structures. The difficulty of identifying reasonable alternative structures, made easy by diagrammatic techniques, is one of the main reasons why complete first-principles studies of this type are rather uncommon. Structural diagrams can also be used to predict the behavior of a pseudobinary system. If the straight line connecting the two points on the diagram representing the end-point compounds crosses a region assigned to a different structure type, the compound might be expected to form in the crossed structure type or a range of heterogeneity may occur. Recent studies on alkaline-earth alloys show the latter behavior.[20]

Another application of the structural diagrams is to predict the unknown structure of a compound with a particular composition or to identify compositions which can form compounds of a particular structure type. For the latter procedure to be complete, however, it must also be determined whether a compound even forms at that given composition. The fact is that while about half of binary combinations which do not form a compound are localized in regions of the diagram labeled "no compound" or "NC," which are not associated with any structure type, the other half are distributed among the regions assigned to the various structure types. While the diagrammatic analysis of compound formation at a particular composition is only an eventual possibility, the less detailed question of compound formation within an alloy system has been studied. One possibility suggested in Ref. 9 is to use the diagrams in conjunction with the Miedema criterion for negative heat of formation. Subsequently, the issue of compound formation has been incorporated into the diagrammatic framework through a three-coordinate scheme, which will be further discussed in Sec. IV.

The three atomic parameter scales—radius, electronegativity, and valence-electron number—contain more information about the compound than just that needed for the structural classification. In a number of cases, such scales have been used for the detailed analysis of quantitative trends in the structural parameters of related compounds. In other words, diagrammatic coordinate scales can be successfully used in the types of analyses commonly associated with crystallographic coordinates. Examples include the analysis of bond lengths in compounds with ZnS, NaCl, and CsCl structures[11] and the pitch angles of the anionic chains in compounds with the CrB structure.[12] In related work,[21] size and electronegativity scales have been used to classify bent-versus-straight triatomic molecules and analyze quantitative trends in the bending angles.

Inherent in these parameters is the possibility for going beyond pure structural analysis to investigate and classify other physical properties of binary compounds. For the *s-p* octet $A^N B^{8-N}$ semiconductors, almost exhaustive structure-property correlations were identified by Phillips and Van Vechten,[5] and many of these (including phase diagrams at high T and high P) have since been confirmed by experiments and by powerful first-principles calculations.[22] However, for more than a decade, crystal chemists have regarded the structures and properties of binary compounds as essentially a closed book, and the cutting edge of research into materials design has concerned ternaries. As we remarked in the Introduction, the properties we will be primarily focusing on—stable quasicrystal formation, high-temperature ferroelectricity, and high-temperature superconductivity—all occur only in ternary compounds. This necessitates an extension of the diagrammatic analysis to ternary systems, described in the following section. In general, the treatment of ternaries is extremely difficult, much more so than binaries, and the results we discuss are the most global generalizations available. Much work still remains to be done.

III. MULTINARY QUANTUM STRUCTURAL DIAGRAMS

The foremost difficulty in extending the diagrammatic method to the study of ternary compounds is the highly incomplete nature of the database. A total of 22 000 binary, ternary, and quaternary compounds are known, to be compared with an estimated 300 000 possible compounds for the ternaries alone (95 284 ternary systems, with an average of 3 compounds per system, for 84 elements excluding noble gases, halogens, and elements with an atomic number higher than 97). This means that at present any analysis based on a statistical approach must be "an extrapolation driven to its limit."[23]

Another fundamental difficulty in applying the method to ternaries is that the generalization of the definition of diagrammatic coordinates for three different constituent elements is not obvious and may not be unique. While coordinates which represent averages of atomic properties are easy to define, the problem of formulating a single coordinate which quantifies size and electronegativity *differences* for three pairs of unlike elements is considerably more subtle. In contrast to the situation in binaries, little assistance can be expected from existing "chemical intuition," as the complexity introduced by adding a third element has significantly hindered its development for ternaries. Indeed, the application of diagrammatic techniques to ternaries may itself prove to play a key role in the development of chemical intuition for these systems.

We first consider the extension of the global organization of crystal structures from binary to ternary compounds. Here, however, we find that there is yet another difficulty. The straightforward generalization of classification into structure types is virtually impossible because ternary structure types are far more numerous than binary types and nearly all have only a few representatives each. More precisely, the 18 000 binary, ternary, and quaternary compounds whose structures have been determined include more than 2200 structure types. Even if we limit ourselves to structure types with at least 2 representatives, we find 16 500 compounds crystallizing

in 650 structure types, which is a substantial increase over the fewer than 100 common structure types needed for the binary-compound subset.

Clearly, "classical" structure type as an organizing principle of ternary-compound structure is of marginal utility. The problem is that the classical structure type contains information in too much detail. This leads us then to seek a classification which is less detailed, but still contains enough information to identify essential similarities or differences between structures. Based on examination of limited subsets of ternary compounds, various general principles governing ternary-compound structures have been proposed in the literature and are summarized in Ref. 23 in the form of nine "rules." Systematic testing of these rules on the full database of structure types shows that only one rule has general validity: that "only structures with a small number of different environments are realized."[24] For each atom in the unit cell, we label its environment type by the coordination number and number of triangles and squares in its coordination polyhedron, which is defined using the maximum-gap method[25] with ambiguities resolved by requirements of convexity and high symmetry. This determination of coordination-environment type is based solely on the geometry of the crystal structure and, furthermore, is rather insensitive to detailed differences, for example, small symmetry-lowering distortions which would change the classical structure type. In fact, with this definition all 650 classical structure types of binary, ternary, and quaternary compounds, even those with more than 100 atoms per unit cell, have 4 or fewer coordination environments. The simplest case is that of the 47 structure types with 2511 binary, ternary, and quaternary representatives which have a single coordination environment. These include many familiar structure types, such as NaCl, CsCl, and ZnS. Approximately 400 structure types with about 10 000 representatives have only 2 coordination environments, and roughly 200 structure types with about 4000 representatives have 3 or 4 coordination environments.

In the following diagrammatic analysis, we explore the idea that the purely geometrical grouping of classical structure types into "general" structure types according to coordination environments should reflect similarities in the chemistry of representative compounds. First, we construct diagrams for the simplest case of the single coordination-environment compounds, where this connection should be most apparent. Examination of the 47 single coordination-environment structure types, with 2511 known representatives, shows that the total number of different coordination environments is surprisingly small. We can group the classical structure types with the same coordination environments into a total of 8 general structure types. Moreover, only the 5 environments shown in Fig. 3 are needed to construct 44 out of the 47 types which include 2483 representatives (99%). For the single coordination-environment compounds, these 5 general structure types provide the global organizing principle for diagrammatic analysis.

It remains to identify the optimal diagrammatic coordinates for efficient separation of the five main general structure types. The definitions are based on the diagrammatic coordinates used in the structural analysis of binary compounds (size and electronegativity difference and valence-electron sum) with two modifications. First, since the number of possible stoichiometries increases greatly for ternaries, the stoichiometry should be included in the coordinate definition, making it possible to include all compounds in a single diagram. For binaries, an appropriate choice is

$$\begin{aligned} \bar{N}_v &= xN_{v,A} + yN_{v,B} \ , \\ \overline{\Delta X} &= 2x(X_A - X_B) \ , \\ \overline{\Delta R} &= 2x(R_A - R_B) \ , \end{aligned} \tag{1}$$

for A_xB_y with $x \leq y$ and $x+y=1$. These definitions are closely related to the QSD coordinates. In fact, ΔR and ΔX are simply rescaled, which tends to preserve the structure type separation for fixed stoichiometric ratio discussed in Sec. II. The use of x as the scale factor naturally distinguishes compounds with the same constituent elements, but different stoichiometry. More surprisingly, we shall see below that this linear scaling also leads to the

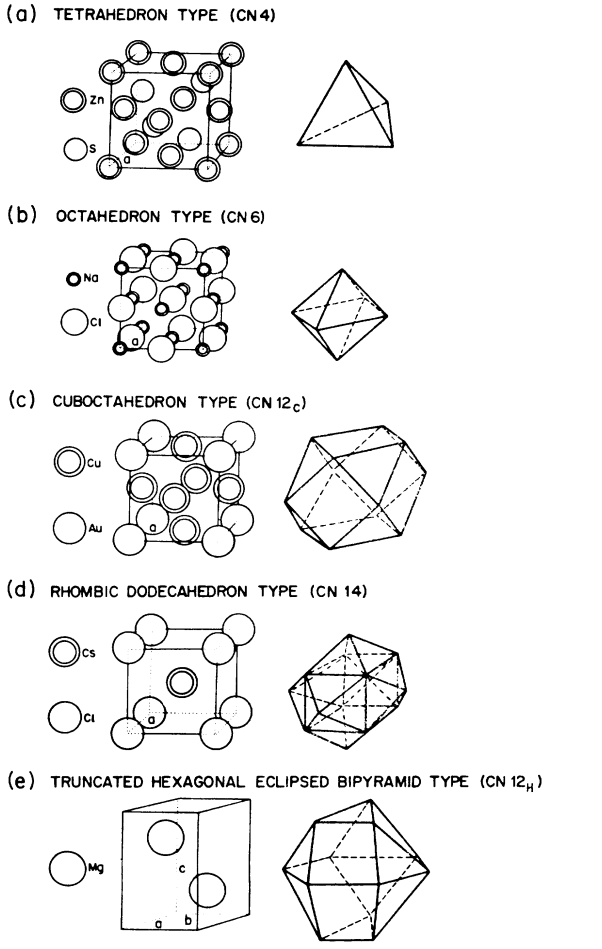

FIG. 3. Representative classical structure type and characteristic coordination polyhedron are shown for each of the five common general structure types of single-coordination-environment compounds (from Ref. 23).

correct coincidences of compounds with different stoichiometry and the same general structure type.

For ternaries, we need to solve the problem not only of including the stoichiometry, but of correctly generalizing the coordinates describing signed electronegativity and size differences. A good choice turns out to be

$$\bar{N}_v = xN_{v,A} + yN_{v,B} + zN_{v,C} ,$$
$$\overline{\Delta X} = 2x(X_A - X_B) + 2x(X_A - X_C) + 2y(X_B - X_C) , \quad (2)$$
$$\overline{\Delta R} = 2x(R_A - R_B) + 2x(R_A - R_C) + 2y(R_B - R_C) ,$$

for $A_xB_yC_z$ with $x \le y \le z$ and $x+y+z=1$. These definitions reduce, as they should, to the binary definitions of Eqs. (1) for $x \to 0$. Quaternaries can be included by averaging the atomic parameters of the two most electronically similar elements (s, p, d, and f) and using the coordinate definitions for ternaries.

Construction of the diagrams using these coordinates and simple separation surfaces for the 2483 compounds into 5 general structure types results in 66 violations (2.7%). As for the binary diagrams,[9] these errors are listed[23] and they exhibit no obvious pattern. Overlaps are permitted only if there are compounds in that region which crystallize in both structure types. Two examples[23] of single coordination-environment QSD's are shown in Fig. 4, corresponding to average number of valence electrons $\bar{N}_v = 6.50$ and 5.00, respectively. For $\bar{N}_v < 3.75$ the diagrams show a very close reflection symmetry across $\overline{\Delta R} = \overline{\Delta X}$. Such a symmetry makes the ambiguity present in the definition of binary coordinates for $x = y$ and of ternary coordinates when any two or all three of x, y, and z are equal irrelevant to structure type determination. However, as $\bar{N}_v$ increases above 3.75, directional valence hybridization is important and the diagrams become markedly less symmetric. Thus, for optimum separation, a particular resolution of the ambiguity in the coordinate definition is indicated by the diagram. Future examination of individual cases may help to clarify the physical interpretation of this process of selection. This change in symmetry also has interesting implications for the structural relationship of "formula conjugates" such as the pair A_mB_n and A_nB_m when $N_{v,A} = N_{v,B}$. For $N_{v,A} = N_{v,B} < 3.75$, the formation of structural antitypes is expected, while for $N_{v,A} = N_{v,B} > 3.75$, this is much less likely to occur. Again, examination of individual cases should prove instructive.

The same QSD coordinate definitions have been used to construct diagrams for two-, three-, and four-

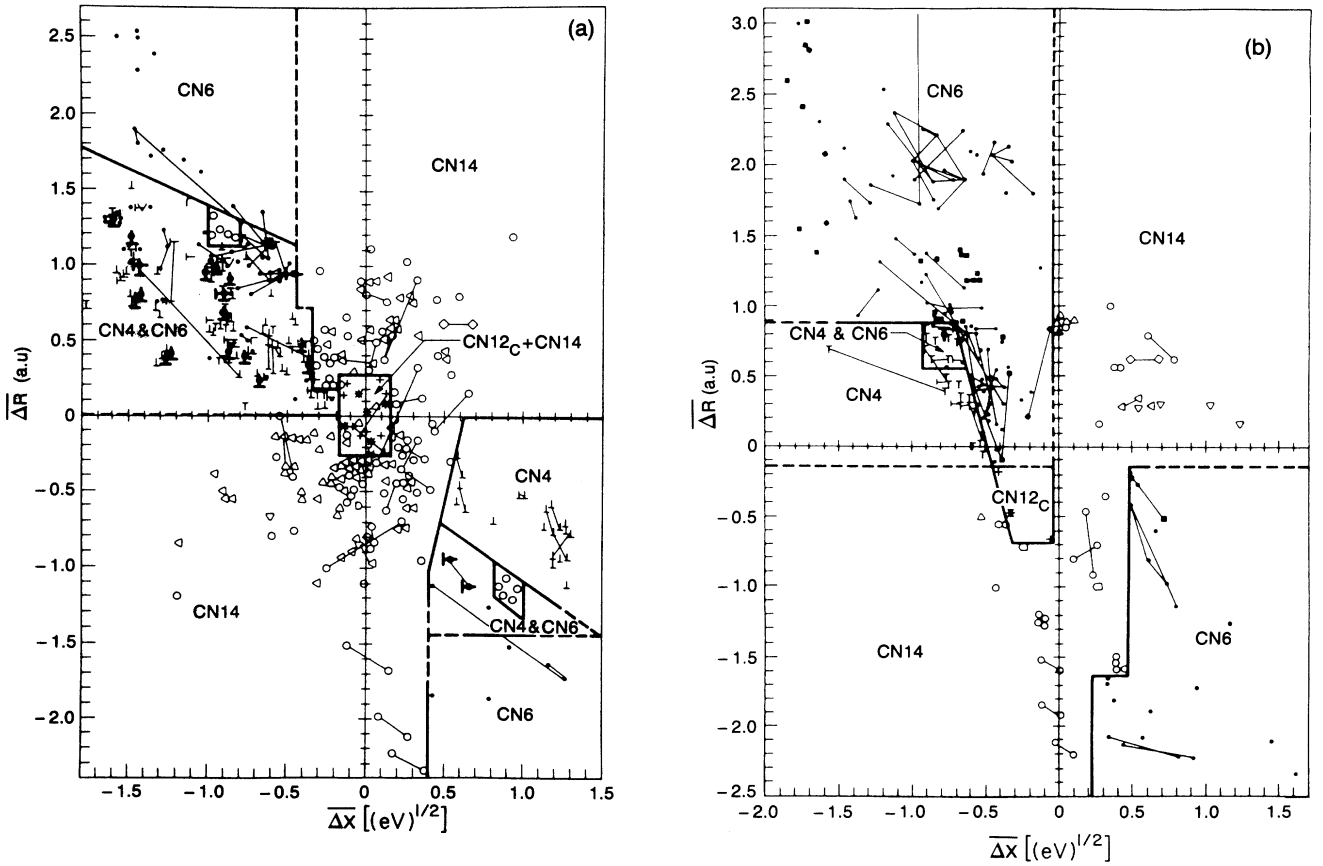

FIG. 4. (a) Quantum structural diagram (QSD) showing the separation between single-coordination-environment binary, ternary, and quaternary compounds, with size and electronegativity differences defined in Sec. III, in a cross section corresponding to $6.25 \le \bar{N}_v < 6.75$. (b) As in (a), but with $4.75 \le \bar{N}_v < 5.25$. The lines represent compounds which occur over a concentration range; further details are in Ref. 23.

coordination-environment binary compounds.[26] For three- and four-coordination-environment compounds, we label the general structure type by the two highest-symmetry coordination environments. In most cases the others can be viewed as lower symmetry "connecting polyhedra," geometrically required by the combination of the two main coordination environments. Excellent separation of general structure types is obtained if different diagrams are used for the two-, three-, and four-coordination-environment cases, i.e., 95%, 98%, and 99%, respectively. The reduction in the number of "general" structural types from the "classical" total is not so dramatic as for single-coordination-environment compounds: 37 general types from 51 classical types for two-coordination-environment binary compounds; 29, from 34, for three; and 19, from 28, for four. However, it is natural to suppose that, as for the single-coordination-environment case, ternaries, and quaternaries can be included in the same diagram as the binaries. This extension should introduce many new classical structure types, but few, if any, new general structure types, greatly increasing the relative effectiveness of this classification.

The quantitative success of the coordination-environment diagrams suggests that the most closely related aspects of crystal geometry and chemistry are accurately represented by the general structure type and QSD coordinates, based on valence-electron number, electronegativity, and pseudopotential core radius. In general, the physical properties of a compound might be expected to depend on features of the geometry and chemistry not included in the diagrammatic description. However, as we shall see in Secs. V, VI, and VII, stable quasicrystals, high-T_C ferroelectrics, and high-T_c superconductors are found to cluster each into localized regions of the QSD. This will lead us to speculate that the underlying physics of these particular properties is intimately related to the presence of certain general structural features.

The picture is, however, incomplete in that it cannot explain why these properties occur only in ternary compounds. Indeed, the single-coordination-environment diagrams directly imply that general structure type is insensitive to any differences between binaries and ternaries. In the next section of this paper, we discuss the question of compound formation in alloy systems. In these diagrams there turns out to be a pronounced difference in the behavior of binary and ternary intermetallic systems. This difference will play a key role in the subsequent discussion of stable quasicrystals.

IV. COMPOUND FORMATION IN BINARY- AND TERNARY-ALLOY SYSTEMS

An alloy system is said to be compound forming whether it contains a single compound or many. It is compound nonforming only if it fails to form a true compound (neither pseudoelemental or, in case of ternary systems, pseudobinary) at any stoichiometry. The systematization and prediction of compound formation has a long and interesting history, summarized in Ref. 27, which included efforts by Hildebrand and, later, Mott to predict binary-liquid immiscibilities. Work on related issues continued throughout the 1970's, the most notable being the definitive study of Miedema on alloy heats of formation.[28] However, these approaches have been limited to binary-alloy systems. In contrast, QFD's developed for the study of binary-alloy systems in Ref. 27 can be extended naturally to ternary systems, and the diagrammatic survey in Ref. 29 is a systematic treatment of compound formation in ternary systems. The observed regularities and the differences between binary and ternary systems form the subject of the rest of this section.

Extensive experimental investigation in binary-alloy systems has resulted in a database of 1967 systems (1384 compound-forming systems and 583 with no compounds), representing 56% of the 3486 possible combinations (excluding H, the halogens, the noble gases, and elements with atomic number greater than 97). Such a database provides a solid basis for diagrammatic analysis. Unfortunately, proportionately far less experimental information is available about the behavior of the 95 284 ternary systems. Furthermore, the data favor compound-forming systems, since compound formation can be established simply and directly from a small amount of experimental data, while an exhaustive study of the phase diagram is required to establish compound nonformation. Thus, while 5048 systems have been shown to be compound forming, compound nonformation has been confirmed in only 550 systems. However, using the empirical rule that no compound will form in a ternary system all of whose binary systems are compound nonforming, an additional 1602 systems can be added to the database of compound nonformers, bringing the total to 2152. The resulting set of 7200 systems, while much larger than the binary database, contains less than 8% of all possible ternary systems, and as in the previous section, we are in a situation of rather extreme extrapolation.

The definition of appropriate diagrammatic coordinates for the separation of compound-forming from compound-nonforming systems is based on the examination of binary systems. Statistical analysis of different combinations of atomic parameters from the five classes (A–E) of trends with atomic number for separation efficiency[27] in the "significant subset" of binary combinations of isostructural elements yielded three coordinates: the size difference $|\Delta R|=|R_A-R_B|$ (class A), the elemental melting point ratio T_A/T_B, where $T_A>T_B$ (class C), and the valence-electron-number difference $|\Delta N_v|=|N_{v,A}-N_{v,B}|$ (class E). Out of 707 experimentally investigated isostructural systems with 467 not forming compounds, the diagram has 28 violations (4%). For 1260 nonisostructural systems with 116 compound nonformers, with the same coordinates (but different separation surfaces) the diagram has 36 violations (3%). In addition, it is possible in these diagrams to separate different types of noncompound phase diagrams (solubility, insolubility, eutectic, and peritectic) with 90% accuracy.[27]

These binary diagrammatic coordinates have a straightforward generalization to the ternary case:

$$\langle|\Delta R|\rangle\equiv(|(\Delta R)_{AB}|+|(\Delta R)_{AC}|+|(\Delta R)_{BC}|)/3\ , \quad (3a)$$

$$\langle T_> / T_< \rangle \equiv (T_A/T_B + T_A/T_C + T_B/T_C)/3 \ , \tag{3b}$$

where $T_A > T_B > T_C$

$$\langle |\Delta N_v| \rangle \equiv (|(\Delta N_v)_{AB}| + |(\Delta N_v)_{AC}| + |(\Delta N_v)_{BC}|)/3 \ . \tag{3c}$$

Examination of the ternary coordinate definitions shows that $\langle |\Delta R| \rangle$ and $\langle |\Delta N_v| \rangle$ depend only on the difference of the extremal values of R and N_v, respectively, and not on the intermediate value. However, different ternary systems generally still have distinct coordinates since the extremal pair of elements are not necessarily the same for R and N_v, and the third coordinate $\langle T_> / T_< \rangle$ depends on the melting temperatures of all three elements. Construction of these diagrams using these coordinates, without any further adjustment, yields an overall separation accuracy of 94%. More specifically, 281 out of 5048 compound-forming systems (5.5%), 22 of 550 experimentally confirmed compound-nonforming systems (4%), and 148 of the 1602 additional candidates for compound nonformation (9%) are misplaced on the diagram. Unlike the binary case, the distinction between isostructural and nonisostructural element combinations appears to be irrelevant, and a single diagram suffices for all cases.

Examination of the shapes and locations of the compound-forming and compound-nonforming regions in the diagrams and of the number of systems in each region of the QFD can be used to deduce general trends suitable for discussion and interpretation. For nonisostructural binary systems, to a first approximation (in fact, better than 90%) all systems are compound forming. For isostructural binary systems, we can say with better than 80% accuracy that all systems with $|\Delta N_v| \leq 3$ are compound nonforming and all with $|\Delta N_v| > 3$ form compounds. In this approximation, $|\Delta R|$ and $T_> / T_<$ are irrelevant, and the details of the complete binary QFD are complicated, showing no general features as a function of these coordinates. In comparison to the binary QFD, the behavior of the ternary QFD is very much simpler. The compound-nonforming region extends out along each axis of the diagram, as shown in Fig. 5. Thus all three coordinates enter into the first approximation: If any two coordinates are small, then the system is compound nonforming, independent of the value of the third. Conversely, if two coordinates are large, the system forms compounds no matter what the value of the third. Constant-($\langle |\Delta N_v| \rangle$) cross sections, illustrating the difference between small and large values of the coordinate $\langle |\Delta N_v| \rangle$, are shown in Fig. 6.

The trends in binary-compound formation can to a limited extent be interpreted as follows. The difference between isostructural and nonisostructural combinations certainly arises from differences in the boundary conditions of crystallites of the elements, favoring compound formation for unlike combinations. In the same way, a large difference in N_v also seems to be a dissimilarity which induces compound formation even in the isostructural case. In principle, the interpretation of the binary QFD can be carried further (perhaps even to the detailed features) by utilizing other theoretical work on alloying behavior. This type of analysis, however, is quite involved and will not be discussed here.

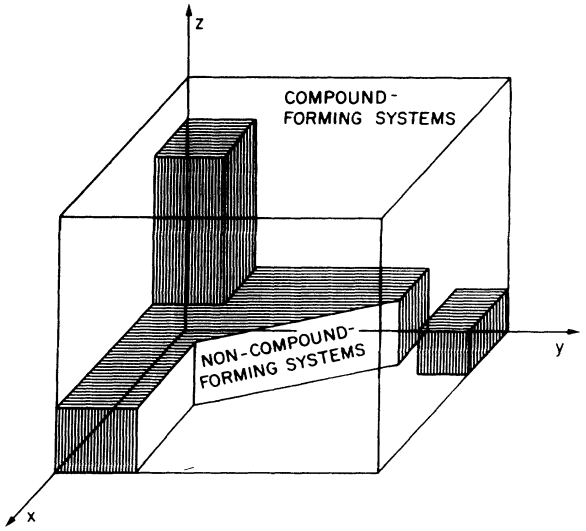

FIG. 5. Three-dimensional quantum formation diagram (QFD), showing schematically the separation into compound-forming and compound-nonforming regions, taken from Ref. 29. The coordinates x, y, and z are defined by Eqs. (3a), (3b), and (3c), respectively, and the Cartesian-axis origin is at (0,1,0).

Lacking theoretical groundwork of any kind, we shall have even less to say about the interpretation of the ternary QFD. Since the ternary coordinates are just the averages of the coordinates of the three constituent binary systems, we can try to identify some relationship between binary and ternary behavior. The empirical observation that compound-nonforming constituent binary systems produce a compound-nonforming ternary system, while the presence of lots of binary compounds is generally associated with lots of true ternaries, should also be of assistance. Though such a simple analysis can rationalize the compound-nonforming region along the $\langle |\Delta N_v| \rangle$ axis, unfortunately it is impossible to deduce the ternary $\langle T_> / T_< \rangle$ and $\langle |\Delta R| \rangle$ dependence which is lacking in the binaries. A more detailed study focusing on ternary systems is needed to resolve this.

The fact that the diagrammatic analysis of compound formation is much simpler in the ternaries than in the binaries may seem surprising. After all, we have repeatedly stressed that the addition of a third element makes ternaries immensely more complex than binaries. However, this reasoning also suggests that the elements should be simplest of all. In fact, investigation of a problem such as crystal structures of the elements shows that almost every case is exceptional, with quantum-mechanical effects relating to the Fermi surface or directional bonding playing crucial roles. At least in a statistical sense, it seems that as the number of different constituent elements in the system grows, the relative importance of these exceptional effects decreases and the effectiveness of the diagrammatic description increases correspondingly.

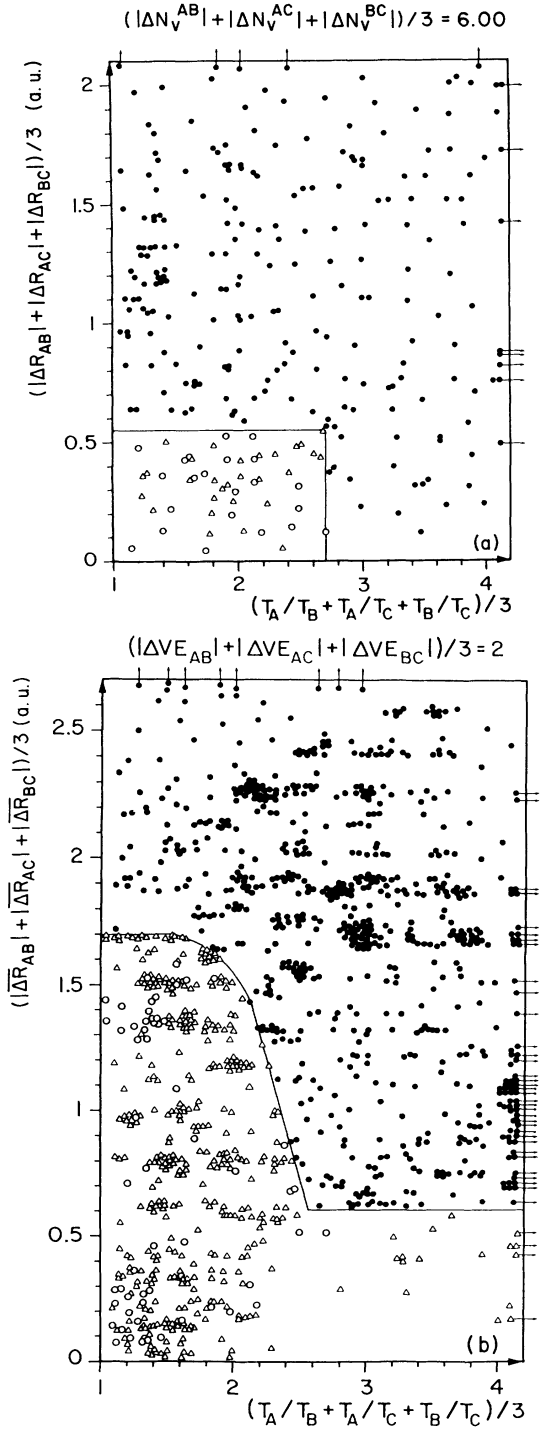

FIG. 6. Constant-$(\langle|\Delta N_v|\rangle)$ cross section of the quantum formation diagram for ternary-alloy systems, with $\langle|\Delta N_v|\rangle=6.00$. A simple boundary can be drawn separating systems which form true ternary compounds (solid circles) from those which do not (open symbols). Systems in which compound nonformation has been established experimentally are designated by open circles. Systems in which compound nonformation was deduced using the empirical rule described in the text are designated by open triangles. (b) Similar to (a), but with $\langle|\Delta N_v|\rangle=2.00$. Note the more complex curve which separates compound-forming from compound-nonforming ternary systems.

In the remainder of this paper, we will be using the quantum diagram technique to study stable quasicrystals, high-T_C ferroelectrics, and high-T_c superconductors. As discussed above, general structural features of these compounds can be studied through the QSD construction. The QFD is, on the whole, less informative, since it describes compound formation in the whole alloy system, rather than at some particular composition of interest. However, systems in the compound-nonforming region might exhibit conflicting structural tendencies at all stoichiometries which inhibit compound formation. If a compound does form in such a system, it is the result of some compromise or exceptional energy factor and, thus, is subject to lattice instabilities, which in turn can be associated with these exotic properties. Intriguingly, most stable-quasicrystal-forming systems are violators of the ternary QFD, as will be discussed in the next section.

V. TERNARY QUASICRYSTALS

Quasicrystals, with their icosahedral symmetry and sharply peaked diffraction patterns, have attracted much attention because they suggest, contrary to long-standing dogma, that icosahedral symmetry can be compatible with long-range translational order. Many metastable quasicrystals have been observed in both binary- and ternary-alloy systems,[30] which generally contain in addition a variety of complex intermetallic compounds and glassy alloys.[31] These include many binary Al-T alloys [T=Mn,[32] Fe,[32] Cr,[32] Ru,[33] V,[33] W,[33] Mo,[33] and Ni (Ref. 34)] as well as $Mg_{32}(Al,Zn)_{49}$,[35] Mg_4CuAl_6,[36] $AuLi_3Al_6$,[37] $Zn_{17}Li_{35}Al_{51}$,[37] and $Ag_{15}Mg_{35}Al_{50}$.[37] In addition, there are quasicrystals which do not contain Al: $(Ti_{1-x}V_x)_2Ni$,[38] Ti_2Fe,[39] Mn_3Ni_2Si,[40] $V_{41}Ni_{39}Si_{23}$,[41] and Cd-Cu.[42]

The metastable examples generally have long-range icosahedral orientational order, while the correlation length for the translational order is typically a few hundred angstroms or less.[43] However, Penrose tiling[44] and, more importantly, techniques of projection from higher-dimensional spaces[45] show that, in principle, icosahedral orientational order is completely compatible with *infinite-range* quasiperiodic translational order. The observed short range for the translational order has been variously interpreted either as an indication that long-range translational order was not inherently favorable[46] or as merely a reflection of the limitations of the fast-quenching preparation technique.[47] The discovery of stable ternary quasicrystals, including $CuLi_3Al_6$,[48] $Ga_{20}Mg_{37}Zn_{43}$,[49] $A_{15}Cu_{20}Al_{65}$ (A=Fe,Ru,Os),[50] $Cu_{15}Co_{20}Al_{65}$,[51] $Co_{15}Ni_{15}Al_{70}$,[51] and (Mn,Re)Pd_2Al_7,[52] with the production of highly ordered micrometer-sized single crystals of $Fe_{15}Cu_{20}Al_{65}$,[53] has proved that there are cases in which long-range quasiperiodic order is favorable in real alloy systems.

In the rest of this section, we will use the quantum diagram technique to establish the nature of the chemical factors promoting quasicrystallinity by identifying regularities in the relatively small set of quasicrystalline materials within the context of the full intermetallic database. With the QSD we can establish a relationship be-

tween quasicrystals and crystalline compounds with icosahedral local coordination environments. In the QFD the quasicrystal-forming ternary-alloy systems are associated with systems in which the formation of true ternary compounds is inhibited. These observations permit the prediction of candidate compositions for new quasicrystals either through straightforward quantitative comparison of diagrammatic coordinates, as in the analysis of Ref. 54, or with strategies based on physical interpretation of the diagrammatic regularities, described in this section and in more detail in Refs. 55 and 56, which are at the same time more exclusive and more general.

The construction of the quasicrystal diagrams proceeds straightforwardly with the computation of the coordinates using Eqs. (2), (3), and Fig. 1 (resulting values listed in Table I) and the plotting of the new points on the full intermetallic QSD and QFD. In Fig. 7 we plot the stable quasicrystals on the QSD. We show $\overline{\Delta R}$ vs $\overline{\Delta X}$, with points projected along $\overline{N}_v$. The stable quasicrystals are localized (into a region near the origin) to an even greater degree than the compounds in the closely related *cI*162 structure type contained in the triangle partially shown with dashed lines (Ref. 54). This is all the more remarkable in that they represent several distinct types of quasicrystals not all corresponding to a single structure type. In Fig. 8 are shown the sections of the QFD containing the systems represented in the stable quasicrystal database. In the $\langle|\Delta N_v|\rangle=6.67$ section, (Ga,Mg,Zn) is very close to (Cu,Li,Al), and both lie essentially on the boundary of the compound-forming region. The three systems which contain the $A_{15}Cu_{20}Al_{65}$ quasicrystals appear on the $\langle|\Delta N_v|\rangle=5.33$ diagram. For A=Ru and Os, the systems fall in the compound-forming region near the boundary, while (Al,Cu,Fe) falls well inside the compound-nonforming region, at virtually the same point as (Al,Co,Cu). Similarly, in the $\langle|\Delta N_v|\rangle=4.66$ section, the systems containing $MnPd_2Al_7$ and the decagonal quasicrystal $Ni_{15}Co_{15}Al_{70}$ are found in the compound-nonforming region, while (Re,Pd,Al) is just outside.

Even at this relatively incomplete stage of the analysis, the prediction of new quasicrystals can be attempted. Four new metastable quasicrystals $Ag_{15}Mg_{35}Al_{50}$, $Zn_{15}Li_{35}Al_{50}$, $Au_{15}Li_{35}Al_{50}$, and $Ga_{15}Mg_{35}Zn_{50}$ and one related stable quasicrystal $Ga_{20}Mg_{37}Zn_{43}$ were successfully predicted[37] by the preliminary quantum diagram analysis of Ref. 54. The database used contained $CuLi_3Al_6$, at that time the only known stable quasicrystal, $Al_{25}Mg_{36}Zn_{38}$,[36] and $Cu_9Mg_{36}Al_{55}$,[37] two metastable ternary quasicrystals, and the ten compounds in the *cI*162 $Al_5Mg_{11}Zn_{11}$ structure type, closely related to these three quasicrystals. From the distribution of these materials on the QSD and QFD, a set of diagrammatic conditions for stable quasicrystals was formulated: (i) the QSD coordinates should lie within the $(\overline{\Delta R})$-$(\overline{\Delta X})$-$\overline{N}_v$ region defined by the three quasicrystals and ten *cI*162 compounds (partially shown by the dashed lines in Fig. 7), and (ii) the ternary-alloy system should lie on the QFD as close or closer to the boundary between compound-forming and compound-nonforming regions than Cu-Li-Al. To narrow the final candidate list to 55 compositions, restrictions were added imposing strong chemical similarity to *cI*162 compounds. It should be noted that the latter restrictions alone, without the use of diagrams,

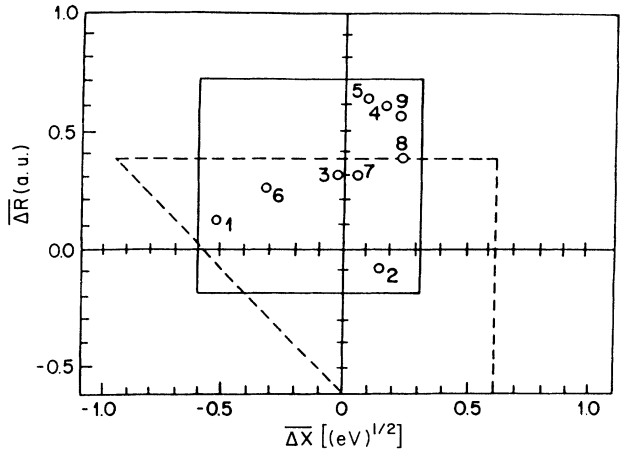

FIG. 7. Distribution of the nine stable quasicrystals on the QSD, projected along the $\overline{N}_v$ axis. Numbering of stable quasicrystals is as in Table I. The dashed line shows a portion of the boundary of the $(\overline{\Delta X})$-$(\overline{\Delta R})$ box defining the quasicrystal QSD condition of Ref. 54, based on *cI*162 compounds and corresponding quasicrystals only. The solid line shows the box used in the present analysis.

TABLE I. Six diagrammatic coordinates used in the QSD and QFD analysis of the nine known stable quasicrystals. N_v' is a modified valence-electron-number scale which includes the filled d-electron shell in the near-noble-metals Cu, Zn, Ag, Cd, Au, and Hg.

		$\overline{N}_v$	$\overline{\Delta R}$	$\overline{\Delta X}$	$\langle\|\Delta N_v'\|\rangle$	$\langle T_>/T_<\rangle$	$\langle\|\Delta R\|\rangle$
(1)	$Cu_{10}Li_{30}Al_{60}$	2.20	0.12	−0.52	6.67	2.15	0.29
(2)	$Ga_{20}Mg_{37}Zn_{43}$	2.20	−0.10	0.16	6.67	2.24	0.22
(3)	$Fe_{15}Cu_{20}Al_{65}$	3.35	0.30	−0.04	5.33	1.71	0.30
(4)	$Ru_{15}Cu_{20}Al_{65}$	3.35	0.59	0.15	5.33	2.29	0.62
(5)	$Os_{15}Cu_{20}Al_{65}$	3.35	0.62	0.07	5.33	2.81	0.65
(6)	$Cu_{15}Co_{20}Al_{65}$	3.90	0.25	−0.33	5.33	1.69	0.24
(7)	$Ni_{15}Co_{15}Al_{70}$	4.95	0.30	0.07	4.67	1.74	0.34
(8)	$MnPd_2Al_7$	4.80	0.37	0.25	4.67	1.74	0.52
(9)	$RePd_2Al_7$	4.80	0.56	0.26	4.67	2.66	0.67

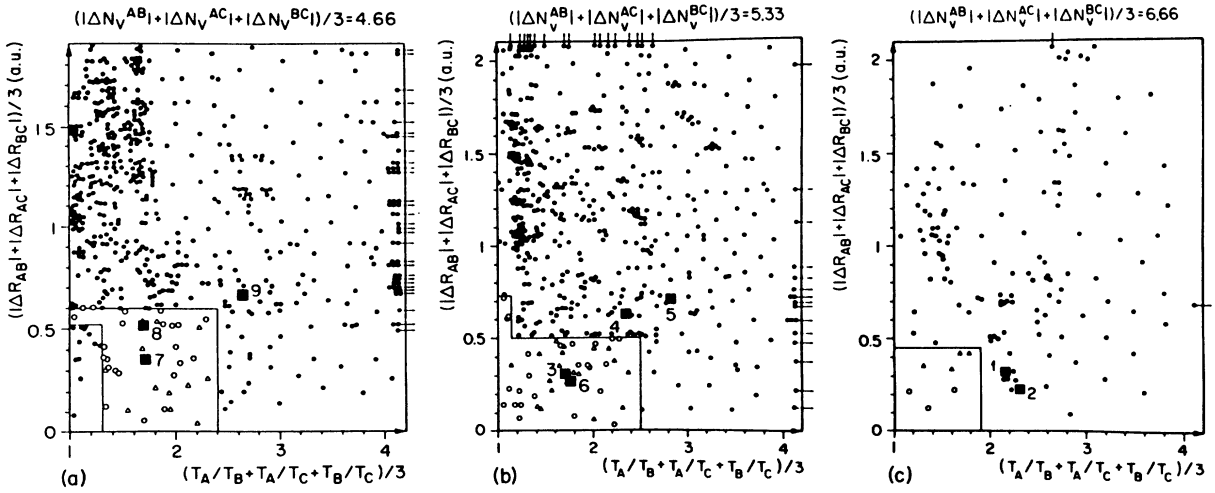

FIG. 8. (a) $\langle|\Delta N_v|\rangle = 4.67$ section of the ternary QFD (Ref. 29), showing the distribution of stable quasicrystals in relation to the boundary separating compound formation (solid circles) from compound nonformation (open circles and triangles). The numbers adjacent to the solid squares identify the quasicrystals as listed in Table I. (b) Same as (a), with $\langle|\Delta N_v|\rangle = 5.33$. (c) Same as (a), with $\langle|\Delta N_v|\rangle = 6.67$.

yield an unwieldy list of 2600 candidate compositions.

In the further development of diagrammatic conditions and prediction strategies for quasicrystals, we will critically examine and draw on some intuitive ideas on quasicrystal formation which have emerged, since their discovery in 1984. At finite temperature the free-energy difference determines the relative stability of crystalline and quasicrystalline phases. Configurational entropy has been much discussed as a factor responsible for stabilizing quasicrystalline structures.[57] In fact, this contribution is very small and should only play an important role when other enthalpic factors are very close to equal.[58] Instead, the primary condition for quasicrystalline formation may be an energetic one, requiring an unusual borderline situation in which a nonperiodic structure is so close in energy to periodic alternatives that subtle chemical energies or entropy differences can swing the free-energy balance in its favor. For this to occur, it should be that local icosahedral order is energetically favored, while the energy gains associated with periodicity in related crystalline structures are small. These ideas can be formulated more precisely, as follows.

The first general principle (I) is that *long-range quasicrystalline order is driven by a tendency to local icosahedral order.* This principle is the basis for the search for new quasicrystals through the modification of known crystalline compounds with a high degree of local icosahedral arrangement,[59] in particular the Frank-Kasper phases.[4,60] Indeed, many (though not all) known quasicrystals do have relationships to such crystalline compounds, in some cases even leading to proposed local atomic arrangements based on the decorations extracted from the known crystal structures regarded as periodic tilings[61] or "rational approximants." This principle also forms the basis for nearly all model systems constructed to exhibit quasicrystalline ground states.[62] The second general principle (II), which is equally important and stated here explicitly, is that *long-range quasicrystalline order is possible only with the suppression of factors favoring long-range periodic order.* Thus local icosahedral order can successfully induce quasicrystal formation only if no favorable crystalline structure exists as an alternative. On the other hand, it is also important that this suppression not be too strong. The energy gain from long-range icosahedral order may be enough to favor a quasicrystalline structure over a periodic crystal of the same composition, but generally not over an alternative phase separation. From this, we extract general principle III: *quasicrystals form only at a composition close to that of some crystalline compound* (which may be only metastable). Compounds which are related in this way to quasicrystals will be referred to as "corresponding compounds."

As already mentioned above, not all corresponding compounds can be described as rational approximants to quasicrystals. In the case of $Fe_{15}Cu_{20}Al_{65}$, the only known compound of nearby composition is $tP40$ Al_7Cu_2Fe. This structure has Cu and Fe segregated into layers in a relatively open structure,[63] with the coordination numbers being 9 for Fe, 11 for Cu, and 4, 8, and 11 for Al. Although the structural features associated with a quasicrystal are absent, the correspondence is strengthened by the fact that Al_7CoCu_2, the only other compound known to have this structure,[7] has a composition close to that of the stable decagonal quasicrystal $Al_{65}Cu_{15}Co_{20}$. This correspondence is the basis for a new structural model for the $A_{15}Cu_{20}Al_{65}$ (A=Fe,Ru,Os) quasicrystals in which a highly ordered array of layered components relieves the strain generated by the local icosahedral order.[64] This model may explain the longer-range order and high electrical resistivity observed in this class of quasicrystals, which probably also includes *i*-Al_7Pd_2(Mn,Re). Careful investigation of the ternary

phase diagrams should reveal additional stable or metastable layered compounds with compositions close to those of the quasicrystals in this class.

By investigating the distribution of known stable quasicrystals on the QSD and QFD, we are led to formulate general "diagrammatic conditions" which we propose should be satisfied by all stable quasicrystals. It is important to recognize that, because of the very small size of the database, there is a considerable degree of flexibility in the statement of the diagrammatic conditions. Clearly, the ternary compositions which are closest in QSD and QFD coordinates to known stable quasicrystals are the strongest candidates for new quasicrystals. However, diagrammatic conditions which depend solely on the "distance" from known stable quasicrystals are likely to exclude many interesting possibilities, including new types of quasicrystals. Thus we suggest more general conditions which are physically motivated by quasicrystal principles I, II, and III, discussed above. As we shall see, these conditions include significant regions of diagram space where no stable quasicrystal has yet been discovered. With further expansion of the database, these generalized conditions will be tested and further refinements made possible.

First, consider the $(\overline{\Delta R})$-$(\overline{\Delta X})$ plot, projected along $\overline{N}_v$, as shown in Fig. 7. The nine quasicrystals are characterized by their proximity to the origin $\overline{\Delta R}=\overline{\Delta X}=0$, with some possible tendency toward positive values of $\overline{\Delta R}$. For information about the behavior of compounds in this region, we look at QSD structural separations of compounds which, like the established corresponding structure type $cI162$, have four inequivalent local coordination environments. We studied 814 binary and ternary compounds in the four-coordination-environment structure types listed in Ref. 26. As shown in Fig. 9, 270, or 51%, of the 535 compounds with icosahedral environments fall in the quasicrystal $(\overline{\Delta X})$-$(\overline{\Delta R})$ box, while only 7, or 2.5%, of the 279 nonicosahedral compounds have $\overline{\Delta X}$ and $\overline{\Delta R}$ values in this range, showing that this region (independent of $\overline{N}_v$) is primarily associated with the formation of icosahedral compounds. Most of the icosahedral compounds which lie outside the quasicrystal box have up to twice as large positive values of $\overline{\Delta R}$. It is evident that small values of $\overline{\Delta R}$ are even more important to quasicrystal formation than to icosahedral four-coordination-environment compound formation. The good clustering of the quasicrystals suggests that we take a simple $(\overline{\Delta R})$-$(\overline{\Delta X})$ box for this part of the diagrammatic conditions.

Next, we consider the third axis $\overline{N}_v$ in the QSD. As in the analysis of the $cI162$ compounds, we use the lower values of N_v for Cu and Zn because, with Zn the majority element in $Ga_{20}Mg_{37}Zn_{43}$, the noble metals and Al seem to be somewhat interchangeable. Also, as can be seen from a comparison of the two sets of $\overline{N}_v$ values in Table I, this definition gives slightly better localization along $\overline{N}_v$. Substitution within the isoelectronic series T=Fe,Ru,Os for $T_{15}Cu_{20}Al_{65}$ and T=Mn,Re for TPd_2Al_7 does not destroy quasicrystalline order. In the T-Cu-Al alloys, increasing N_v of the transition metal seems to produce a change from icosahedral order in T=Fe,Ru,Os to decagonal in Co. Furthermore, $(T^1)_{0.5}(T^2)_{0.5}Pd_2Al_7$ is icosahedral for (T^1,T^2)=(Cr,Fe), (V,Co), (Mo,Ru), and (W,Os) and decagonal for (T^1,T^2)=(Nb,Rh) and (Ta,Ir).[65] Theoretical studies of Al-Mn have also suggested that electronic energy (and, thus, electron count) might play an important role in structural stabilization.[66] Thus $\overline{N}_v$ clearly is an important parameter in characterizing the tendency to quasicrystal formation for these materials. However, Table I shows values of $\overline{N}_v$ ranging from 2.20 to 4.95, with clustering only for very closely related quasicrystals. As a result, we take a rather loose condition on $\overline{N}_v$, with emphasis on $\overline{N}_v \lesssim 5$, but not excluding higher values from consideration. This is not in contradiction to the observation[67] that many known quasicrystals have a Hume-Rothery "outer electron number" e/a in the vicinity of 1.75, since $\overline{N}_v$ and e/a are computed differently, with empirically determined valences for transition elements such as Mn. However, the Hume-Rothery rule applies only to a severely restricted class of intermetallic compounds.[68] This rule thus cannot aid in the prediction of novel quasicrystals outside this class, while the QSD coordinate definitions are equally valid throughout the entire database.

Our approach to formulating diagrammatic conditions from the QFD contrasts with that based on the QSD in that we make a much more direct connection to the properties described by the QFD. In the full intermetallic

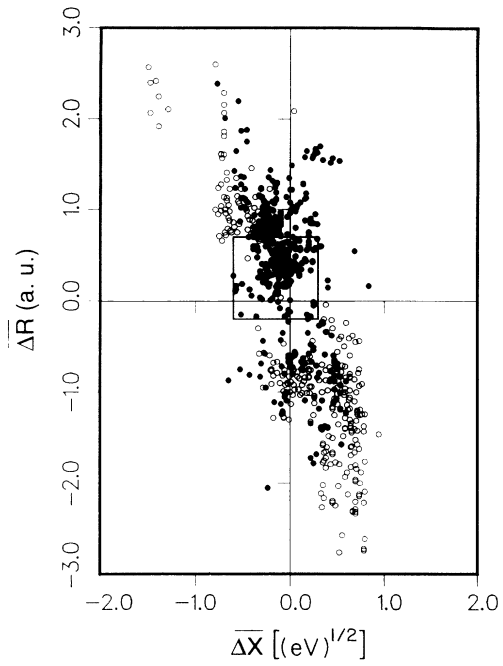

FIG. 9. $\overline{\Delta R}$ vs $\overline{\Delta X}$ for the 814 binary and ternary compounds in the four-coordination-environment structure types listed in Ref. 26. Compounds with an icosahedral coordination environment are indicated by solid circles and nonicosahedral compounds by open circles. The quasicrystal $(\overline{\Delta X})$-$(\overline{\Delta R})$ box is shown by solid lines.

QFD, ternary-alloy systems are grouped according to whether they form compounds or not, and no special significance is in general attached to proximity of two systems within one of these two regions. (In the case of binary systems, compound nonformers can be additionally separated according to the type of phase diagram.) It is then natural in the analysis of the behavior of the quasicrystals in the QFD to apply the same classification, rather than imposing constraints on the actual values of QFD coordinates. From Fig. 8 it is clear that the quasicrystal systems are either in the compound-nonforming regions or close to the boundary. Furthermore, the systems in the compound-nonforming region are actually *violations* of the QFD since they also contain stable ternary compounds, which therefore must either be stabilized by exceptional factors outside the scope of the QFD or be just barely stable, beyond the quantitative accuracy of the QFD. In either case the energy contribution favoring periodicity might generally be expected to be abnormally low. We therefore propose the QFD condition that quasicrystals form in compound-forming alloy systems which are in or near to the compound-nonforming region of the QFD. Compound formation in these systems is an expression of the incomplete suppression of the tendency to form crystalline compounds, which allows the alternative quasicrystal structure, stabilized by local icosahedral order, to become energetically competitive. This condition is the diagrammatic form of quasicrystal principle II.

In the preceding discussion, our attention has been focused on the prediction of ternary quasicrystals. It is also interesting to examine the relevance of this analysis to quasicrystal formation in binary systems. One possibility is that the quasicrystal diagrammatic conditions can be directly translated from the ternary to the binary case. Given the insensitivity of the QSD to the binary-ternary distinction, it is reasonable to expect that the binary-quasicrystal QSD condition might be the same as for ternaries. The QFD condition is more of a problem, since binary[27] and ternary[29] QFD's are so different. We could tentatively formulate the binary-quasicrystal QFD condition as compound formation in proximity to the binary compound-nonforming region. However, the distribution of metastable binary quasicrystals does not provide much support for this. Probably, violation of the binary QFD by compound formation is *not* generally associated with a weakening of the tendency to form periodic compounds, but with other types of exceptional factors such as covalent bonding. In fact, it may be that for binaries the energy gains resulting from formation of periodic structures are generally quite large, overwhelming the energy scales associated with local icosahedral order. This imbalance would be able to account for the lack of known stable binary quasicrystals.

We can test these diagrammatic conditions by checking their validity for known metastable ternary quasicrystals. Since these quasicrystals are observable only as a result of their kinetic behavior, the chemical factors governing their energetics will in general not be as sharply defined. However, the metastable ternary quasicrystals of known composition all nearly satisfy the stable quasicrystal diagrammatic conditions.

The prediction of new ternary quasicrystals is both the most critical test and most useful application of the diagrammatic analysis. In the rest of this section, we give an overview of different prediction strategies and their diagrammatic implementation. Detailed descriptions and prediction lists will be presented separately.[55] A simple prediction strategy is that formulated in Ref. 54, already mentioned previously. A stoichiometric ratio and restrictions on the chemistry of the constituent elements are chosen based on a known quasicrystal, and the resulting large number of combinations are screened using the quasicrystal diagrammatic conditions. The application of such a procedure to the prototype quasicrystals $Fe_{15}Cu_{20}Al_{65}$, $Os_{15}Cu_{20}Al_{65}$, and $Ru_{15}Cu_{20}Al_{65}$ is described in Ref. 55, and this approach has been further developed in Ref. 56.

Next, we discuss the procedure of identifying new "corresponding compounds," for which small modifications in composition may stabilize quasicrystalline order. If QSD coordinates and plots were available for the full intermetallic database, the screening of known compounds using the quasicrystal diagrammatic conditions would be an automatic process. However, since the construction of QSD for multiple-coordination-environment ternary and quaternary compounds is not yet complete, we need to use additional devices to reduce the number of compounds for which coordinates are to be computed.

One such device is to examine only compounds crystallizing in particular structure types. Clearly, structure types corresponding to known stable quasicrystals are the prime candidates for inclusion in this survey. As discussed above, the *cI*162 structure type, corresponding to $CuLi_3Al_6$, contains corresponding compounds for several other stable and metastable quasicrystals. Structure types corresponding to known metastable quasicrystals should also be considered. To extend the analysis even further, structure types for which no quasicrystal formation is yet known, but which exhibit the structural features associated with quasicrystalline order (icosahedral environments, large unit cells), can be included. As is well known, the analysis by structure type alone yields an unwieldy candidate list of many hundreds of compounds, including over 400 Frank-Kasper phases.[7,60] The additional application of the QSD and QFD conditions reduces this number considerably.

Another approach to identifying new corresponding compounds is based on a preliminary screening of alloy systems based on the QFD quasicrystal condition. A list of the ternary-alloy systems located in the compound-nonforming region, which violate the QFD by forming compounds, is readily available.[29] The possible corresponding compounds obtained by applying the QSD conditions to known compounds forming in these systems will not all crystallize in recognizable corresponding structure types. Thus this approach will generate quasicrystal predictions not included in the list based on corresponding structure types. Furthermore, such predictions can be expected to lead to new quasicrystals, based on the precedent of the $A_{15}Cu_{20}Al_{65}$ stable quasicrystals. In that case the only possible corresponding compound of

nearby composition is Al_7Cu_2Fe, with the relatively open $tP40$ structure described above. In fact, it may actually be advantageous for the growth of large, well-ordered samples if the corresponding compound is *not* locally similar to the quasicrystal. For this reason a prediction strategy based on the QFD and not on structure type may be more effective.

Other diagrammatic strategies are possible which do not even use the principle of corresponding compounds. For example, diagrams can be used to identify third elements to be added to binary compounds possessing corresponding structure types. In many cases it has been observed that the addition of even small amounts ($<10\%$) of a third element will significantly enhance quasicrystalline order.[31,69] Another strategy derives from the observation that quasicrystals can form over a range of compositions, with examples such as the pseudobinary $(Ti_{1-x}V_x)_2Ni$ (Ref. 38) and the pseudoternary $Mg_{32}(Al,Zn,Cu)_{49}$.[70] With diagrams, the most favorable elements for substitution into a particular system can be identified, with the possibility even of generating a new binary or ternary by complete substitution.

It is very clear from the discussion in this section that a database of nine examples, though their regularities on the QSD and QFD be very striking, cannot produce a definitive and unambiguous analysis. Even if the stable quasicrystal database were significantly larger, permitting the derivation of stricter diagrammatic conditions, our empirical method simply does not have the resolution to distinguish, say, between quasicrystals and high-order rational approximants. Actual quasicrystal formation is ultimately determined by subtle factors beyond our control, our analysis being designed to identify specific compositions where quasicrystalline structures are competitive in energy with conventional crystalline alternatives. Since the likelihood of quasicrystal formation is then significant, our idea is that the different formulations of diagrammatic conditions and resulting prediction strategies provide a definite direction to the future search for new quasicrystalline materials. The subsequent rapid expansion of the database will then feed back into this analysis, yielding increasingly efficient prediction procedures and a deepening understanding of the classification and physics of quasicrystals.

VI. HIGH-T_C FERROELECTRICS

Ferroelectricity is characteristically a structural property, defined by the presence of atomic displacements giving rise to a uniform electric polarization which can, at least in principle, be switched by application of an external electric field.[71] Like quasicrystallinity, ferroelectricity when originally discovered was thought to be the result of some unique and highly constrained combination of circumstances. However, the past 50 years have seen the discovery of ferroelectricity in a broad range of materials, predominantly various classes of oxides. With very few exceptions ferroelectric compounds contain at least three different elements, thus complicating detailed study.

Significant progress in modeling the behavior of ferroelectric materials was made through the formulation of the "soft-mode" theory. In this theory the transition from a high-temperature paraelectric phase, with zero uniform polarization, to a low-temperature ferroelectric phase occurs as the temperature-dependent frequency of a particular zone-center optic phonon (the soft mode) tends to zero at $T \rightarrow T_C$. Below T_C, the atomic displacements corresponding to the soft mode freeze in, resulting in a nonzero uniform polarization. However, this theory does not address the question of how the anharmonicity necessary to produce the phonon-frequency temperature dependence arises from the chemical and structural features of the material.

A lattice instability such as that of ferroelectricity can reasonably be argued to originate in underlying structural frustration. In an overconstrained high-symmetry structure, such as the perovskite structure possessed by many ferroelectrics, nonideal bond lengths and angles will lead, for energetic reasons, to atomic displacements which vanish for $T > T_C$ because of the vibrational entropy advantage of the high-symmetry structure. However, if the deviations from ideality are too large, then even a distorted version of the structure will be unfavorable compared to other possible structures or phase separation.

The goal of the present analysis is to identify the chemical factors which give rise to this borderline situation in oxide ferroelectrics. Diagrams based on ionic radius scales have been widely used to identify structural regularities within certain classes of oxide compounds.[72] For example, Wood's classic geometrical discussion[73] of ABO_3 compounds (where A is an s-type element), utilized the A and B ionic radii to separate these binary (with $A=B$) and ternary materials into perovskite and other structures, as shown in Fig. 10. The perovskites themselves lie near the upper center of the r_A^i and r_B^i (ionic radii) field, while La_2O_3 is at the extreme right center. However, a search for systematics in monomolecular volumes, shown in Fig. 11, resulted in a great many anomalies. These were inferred to be the results of mixed ionic and covalent bonding and could not be remedied by adjusting the elemental radii.

In the rest of this section, we describe a diagrammatic analysis of ferroelectric compounds,[74] which is intended to go beyond the classical analysis of trends within certain carefully chosen sets of compounds to the global treatment of a wide range of compounds on an equal footing. The same QSD coordinate definitions which lead to the organization not only of the structure of the full database of intermetallic compounds, but of binary oxides and halides as well, are applied to a comprehensive database of oxide ferroelectrics. The striking regularities in the resulting diagram suggest that the QSD coordinates provide a meaningful measure of the structural factors which produce ferroelectricity in these complex compounds. In addition, the diagrammatic organization forms a basis for predicting materials that will exhibit ferroelectricity and other related properties.

To analyze ferroelectricity in oxides, we established several databases by surveying a number of review articles.[75–81] The resulting list contained 72 ternary ferroelectric and antiferroelectric oxides, which we divided

into two sets. The first set F_1, with 50 representatives, contains compounds with $T_C > 500$ K, while the second set F_2, with 22 representatives, contains compounds with $300\ \text{K} < T_C < 500$ K. Finally a third set F_3, with 103 representatives, contains pseudoternary and quaternary ferroelectric and antiferroelectric oxides with $T_C > 500$ K.

Values of the QSD coordinates $\overline{\Delta X}$, $\overline{\Delta R}$, and $\overline{N}_v$ were computed for all three sets of materials. Many of the ternary compositions considered are of the form $A_xB_yO_{1-x-y}$ with $x = y$, resulting in an ambiguity in the definition of size and electronegativity differences in Eqs. (2). We resolve this ambiguity for this class of materials by choosing A through the condition $X_A > X_B$ [i.e., $\overline{\Delta X} = 2x(2X_A - 2X_C)$]. This choice is based both on the empirical observation that the ternaries with $T_C > 500$ K (set F_1) are most tightly localized with this condition and on the physical interpretation that the electronegativity closest to that of oxygen is most important in determining the degree of covalency and thus the tendency towards low-coordination-number distorted structures. The calculation of $\overline{\Delta X}$ and $\overline{\Delta R}$ for the pseudoternaries and quaternaries with $T_C > 500$ K (set F_3) is performed by combining the two most chemically similar constituent elements into a single effective "element" whose properties are the weighted average of the two.

The resulting $\overline{\Delta X}$ and $\overline{\Delta R}$ values for the ternaries, pseudoternaries, and quaternaries with $T_C > 500$ K (sets F_1 and F_3) are confined to a very small portion of the QSD, as shown in Fig. 12. The area occupied by set F_1 is particularly small, while the inclusion of set F_3 requires a slight displacement of the left-hand boundary to larger values of $|\overline{\Delta X}|$.

This figure also shows a Matthias population plot of T_C vs $\overline{N}_v$ for the 153 compounds belonging to the F_1 and F_3 sets. This shows a very narrow peak, even narrower than is found for superconductors, for which such plots are usually made.[82] The narrowness of this peak is consistent with the excellent localization in the $(\overline{\Delta R})$-$(\overline{\Delta X})$ diagram. We used it with the compounds containing ele-

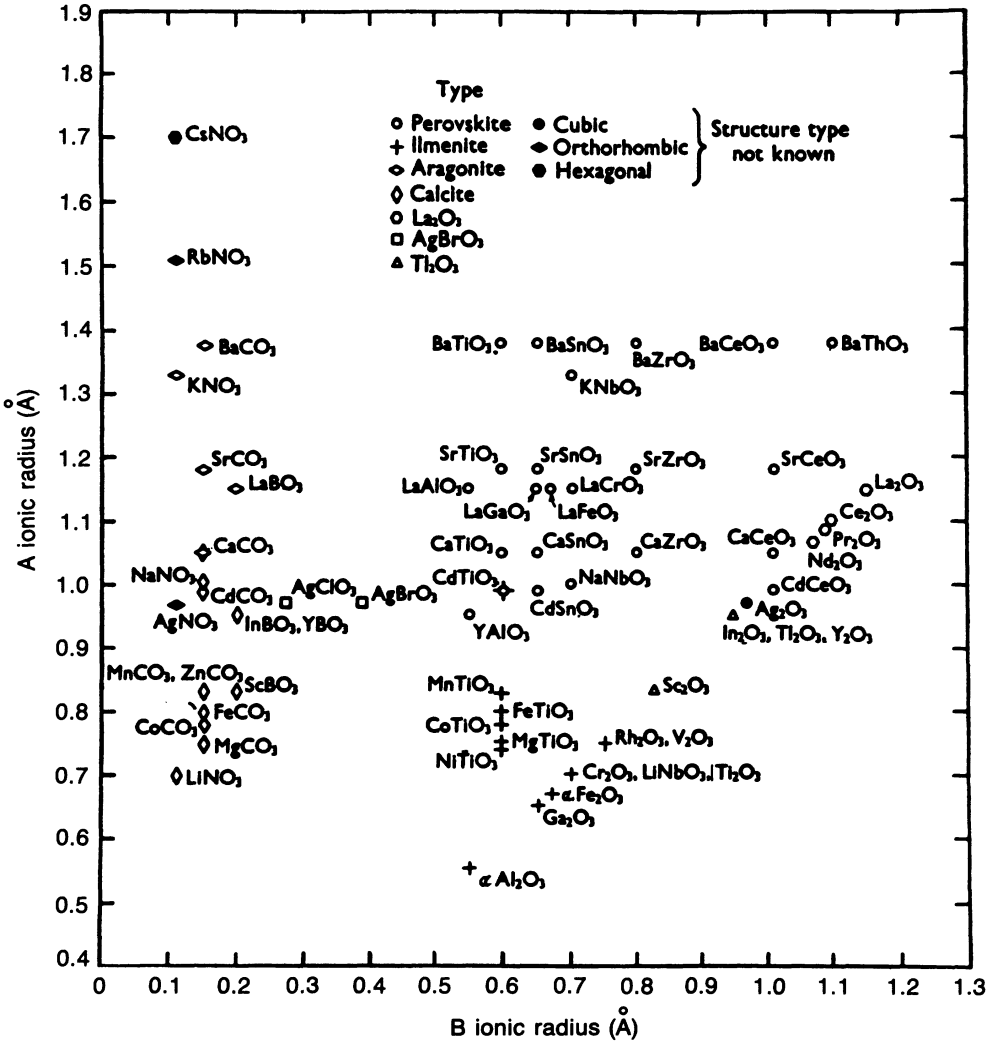

FIG. 10. Classical crystallographic structural diagram of ABO_3 compounds according to ionic radii r_A^i and r_B^i, reproduced here for the reader's convenience from Ref. 73.

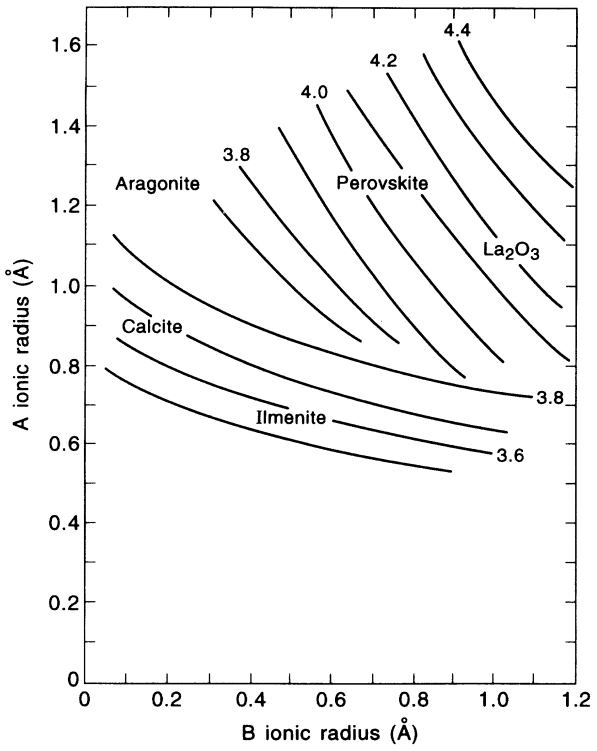

FIG. 11. Monomolecular isovols for the ABO_3 compounds of Fig. 10, adapted from Ref. 73.

ments from the Cu and Zn groups to define $N_v = 1$ and 2 for these elements, respectively, as one would expect for insulators. Finally, we note that this localization is a new result which has not been obtained previously. For the coordinates $\overline{\Delta R}$ and $\overline{\Delta X}$, this is a consequence of the present definition for ternaries, but $\overline{N}_v$ is certainly easy to calculate, and so we were surprised to find a similar localization, hitherto unrecognized, in the ferroelectric Matthias plot.

The localization of the F_1 and F_3 ferroelectrics in the QSD is not a trivial consequence of the localization of certain structure types in which ferroelectricity is prevalent. The 153 (F_1+F_3) compounds are distributed among more than 15 different structure types with many different stoichiometries and are more tightly localized than the full set of compounds in any individual structure type, e.g., perovskite. On the other hand, the degree of localization does significantly depend on the lower bound on T_C reaching a threshold level. The 22 ternary compounds with 300 K $< T_C <$ 500 K (set F_2) are distributed on a QSD volume about 8 times as large as that filled by the 50 ternary compounds with $T_C > 500$ K. At the same time, we find that increasing the lower bound for T_C above 500 K does not significantly reduce the volume occupied by the remaining representative compounds.

The localization of high-T_C ferroelectrics into a single island narrow in all three QSD coordinates $\overline{\Delta X}$, $\overline{\Delta R}$, and $\overline{N}_v$ raises tantalizing questions. In particular, one would like to understand why these and only these values are so favorable for ferroelectricity. A full answer to this question, however, would require a diagrammatic analysis of the full database of insulating ternary and quaternary oxides, in order to put the small subset of ferroelectric materials into their proper context. Perhaps this region is associated with certain low-symmetry coordination environments for oxygen, producing a large local field, or with a high-coordination-number environment under tensile stress for one of the cations, promoting a covalent-ionic instability.

Furthermore, why does T_C play such an important role in increasing localization? A large T_C may be associated with a large low-temperature structural distortion dominated by the relatively simple chemical factors included

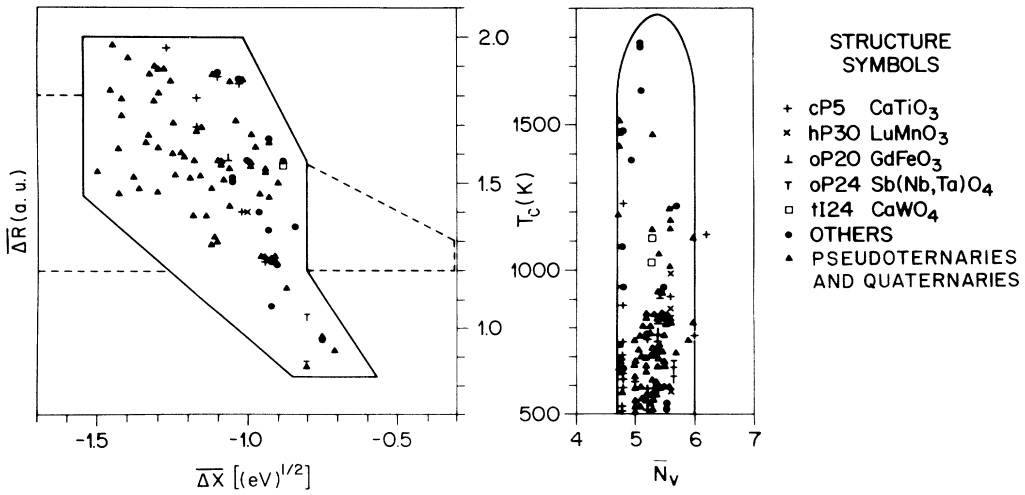

FIG. 12. Quantum structural diagram (QSD) for 153 high-T_C (> 500 K) ferroelectric and antiferroelectric oxides. Pseudoternaries and quaternaries with $T_C > 500$ K (set F_3) are represented by solid triangles; the ternaries with $T_C > 500$ K (set F_1) are represented by a variety of symbols distinguishing different structure types as specified in the legend. The outline for island C from Fig. 13 is indicated by a dashed line to facilitate comparison of ferroelectric with superconducting domains.

in the QSD, while lower-T_C ferroelectric transitions may result from a more subtle balance of structural energies beyond the resolution of this method. There is an interesting connection here to the dimensional classification scheme of Abraham and Keve,[83] where "one-dimensional ferroelectrics," with atomic displacements along the direction of polarization, have higher values of zero-temperature spontaneous polarization than two-dimensional and three-dimensional ferroelectrics, with a more complicated relationship between atomic displacements and the polarization direction. Our high-T_C databases F_1 and F_3 contain predominantly one-dimensional materials, and the diagrammatic localization may in fact be a reflection of this structural classification.

Last, why should ferroelectricity be almost exclusively confined to materials which are at least ternary? As in intermetallic systems, where the QSD made no distinction between binary and ternary compounds, we probably need to look for some analog to the QFD which would describe compound formation in binary- and ternary-oxide systems. From such an analysis it might be found, for example, that "compound-nonforming" ternary systems may find it sometimes more favorable to form a compound in some compromise structure subject to a ferroelectric transition, while a binary system has less stoichiometric flexibility to arrive at such a result.

To end this section, we discuss some preliminary ideas for how QSD localization can aid in the search for new ferroelectric oxides. One approach is to screen known oxide compounds for those which lie in or near to the QSD region defined by the high-T_C ferroelectric database. This search can be performed by computer with the Inorganic Crystal Structure Database,[8] since values of $\Delta\overline{X}$, $\Delta\overline{R}$, and $\overline{N}_v$ are quickly calculated directly from the compound's composition. This database also contains additional information for each compound, such as the Pearson symbol, space group, and lattice constants, permitting further screening, for example, for a noncentrosymmetric low-temperature space group. A search strategy involving screening of known compounds has been previously proposed and implemented by Abrahams;[84] however, it is based on structural criteria requiring a reliable and fairly complete experimental structural determination, while a diagrammatic screening criterion requires only knowledge of the composition.

A compositional criterion has the important advantage that it can be extended beyond the rather incomplete database of known compounds. A particular stoichiometry or set of stoichiometries can be chosen and all possible combinations of elements screened, whether or not a compound of that composition is known or has been characterized. Without some additional screening condition, such a list would probably be too long to be of practical use in the laboratory. For example, a QFD-like condition would provide extra selectivity. More importantly, additional conditions suggested by the known physics of ferroelectrics could, after having been tested on the existing database, be applied in the prediction strategy. This approach would thus simultaneously expand the list of known materials and contribute to an increased understanding of the physics of ferroelectricity.

VII. HIGH-T_c SUPERCONDUCTIVITY

Superconductivity is a dramatic phenomenon in which a metal undergoes a phase transition with decreasing temperature to a zero-resistivity state with unusual magnetic properties. Originally observed in Hg in 1911, superconducting phase transitions have since been found to occur in hundreds of elemental, binary, and ternary materials, though always only at very low temperatures. The highest transition temperature in a pseudoelement (a solid solution whose range of composition includes the pure element) is $T_c = 9.8$ K (Pb-Bi alloys).[85] Materials which are more complex chemically can have significantly larger T_c's. For example, the binary $A15$ compounds show superconductivity at higher temperatures, with $T_c = 23$ K in Nb_3Ge,[85] while the recently discovered ternary and quaternary cuprate superconductors can achieve impressive transition temperatures above 100 K.

Many important features of the superconducting phase transition and zero-resistivity state can be described theoretically through effective field theories which contain phenomenologically determined adjustable parameters. This approach obscures the origin of superconductivity in the chemistry and structure of the relevant materials. The electronic spectrum and electron-phonon interactions, which are central features of conventional superconductors, are intimately related to details of crystal chemistry and the tendency toward lattice instability. Exotic mechanisms, in which interest has recently revived in relation to cuprate superconductors, must also ultimately be rooted in crystal structure and chemistry.

The complexity of superconducting materials increases roughly with T_c, putting high-T_c systems well beyond the scope of thorough first-principles analysis. Indeed, calculations of T_c even for relatively simple elements and compounds are fraught with difficulty. The empirically based diagrammatic approach is thus a valuable tool for the study of chemical trends and features in high-T_c materials. Many useful results have previously been obtained and are described in Ref. 86. In the rest of this section, we review the construction and interpretation of QSD's for high-T_c superconductors, examine the relationship to the high-T_C ferroelectric QSD's of Sec. VI, and describe possible diagram-based approaches to the prediction of new high-T_c superconducting materials.

We divide superconductors into those with high T_c (> 10 K), of which about 70 are known (to which list more high-T_c superconducting cuprates are constantly being added), and those with $1 < T_c < 10$ K (of which about 600 are known). These materials, with their crystal structures, T_c, and, for the high-T_c compounds, $\Delta\overline{R}$, $\Delta\overline{X}$, and $\overline{N}_v$, are listed elsewhere.[85]

For the superconductors with $T_c > 10$ K, the QSD (projected along the $\overline{N}_v$ axis) and the T_c-vs-$\overline{N}_v$ plots are shown in Fig. 13. The compounds are well localized in $\Delta\overline{R}$ and $\Delta\overline{X}$ into three separate islands, labeled A, B, and C, and each island is characterized by particular ranges of $\overline{N}_v$. Island A is dominated by high-T_c superconductors in the $cP8$ Cr_3Si ($A15$) structure, but it contains

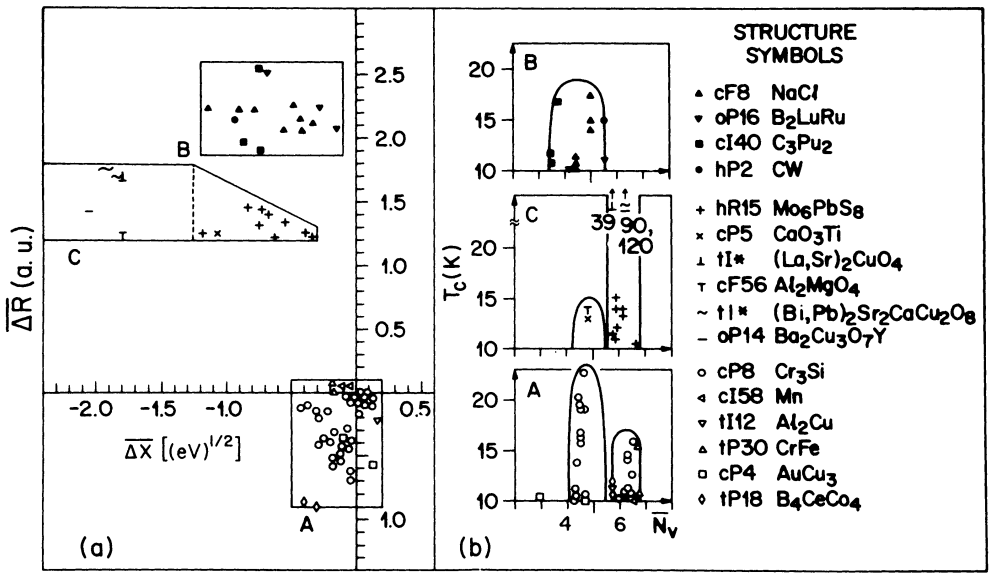

FIG. 13. Quantum structural diagram (QSD) for 67 high-T_c (> 10 K) superconductors, updated from Ref. 86. For the cuprate superconductors in island C, minor differences in the layer compounds (addition or subtraction of one layer) or in substitutional doping shift the points only very slightly.

compounds in five other structures as well. There are $A15$ compounds outside island A with $T_c < 10$ K; i.e., the boundaries of island A contain structural information that in some ways transcends that provided by the common occurrence of high-T_c superconductivity in the $A15$ structure. Similarly, island B is dominated by cubically and hexagonally packed simple AB binaries, but there are *hundreds* of such binaries *outside* island B which are *not* high-T_c superconductors. Finally, island C contains Chevrel, perovskite, and pseudoperovskite cuprate high-T_c superconductors, as well as $LiTi_2O_4$. Perhaps the most obvious feature of island C is that it spans a narrow size range $\overline{\Delta R}$, but a wide range of $\overline{\Delta X}$. Less obvious, but of profound structural importance, is the fact that while binaries dominate islands A and B, all the compounds in island C are ternaries. The imposition of a lower cutoff on T_c is an important factor in producing good QSD localization. The dividing temperature (10 K) is not arbitrary. Since the highest transition temperature in a pseudoelement is $T_c = 9.8$ K (Pb-Bi alloys), one can say that high-T_c superconductive chemistry begins at 10 K. This statement is borne out by our diagrammatic analysis. While the 70 superconductors with $T_c > 10$ K are localized in the A, B, and C islands in Fig. 13, the 600 superconductors with $1 < T_c < 10$ K are scattered uniformly over the entire space spanned by binary and ternary compounds indicated in Fig. 4. In other words, there is something structurally special about superconductors with $T_c > 10$ K which is not shared by superconductors with lower values of T_c.

The division of the high-T_c compounds into three distinct regions on the QSD provides a classification suggesting common features in each class which transcend detailed features of structure types.

On the binary intermetallic QSD, island A is populated by tetrahedrally close-packed metals, a surprising fraction of which are high-T_c superconductors. The close packing, rather than the low-dimensional "chain" structures widely considered to be the basis for high-T_c superconductivity in the $A15$ materials, is the common geometrical feature of superconductors in this island. It is also significant that this island lies at the boundary of the $(\overline{\Delta X})$-$(\overline{\Delta R})$ region occupied by known compounds, with almost no compounds occurring deeper in the $\overline{\Delta X} < 0$, $\overline{\Delta R} < 0$ quadrant.

With a very high value of $\overline{\Delta R}$, nearly all of island B is sparsely populated on the binary intermetallic QSD, and again, a large fraction of the compounds present are high-T_c superconductors. The exception is the low $\overline{N}_v$ portion ($3.75 \leq \overline{N}_v < 4.25$), which contains a large number of nonsuperconducting compounds in the $cF8$ NaCl structure type, while the eight high-T_c NaCl-type compounds are found only at higher $\overline{N}_v$ values. This suggests the idea that a valence-electron count above the "normal" range for the formation of the NaCl structure may be associated with the superconducting instability.

Since island C contains only ternary and quaternary oxides, rather than compare it to the binary intermetallic QSD, we relate it to the ferroelectric QSD constructed in the previous section. To facilitate the comparison, the outline of island C has already been indicated on the ferroelectric QSD in Fig. 12. The $\overline{N}_v$ ranges of the two classes of materials are offset, with the superconductors mostly in the range $5.7 \leq \overline{N}_v \leq 6.7$, while ferroelectrics have $4.7 \leq \overline{N}_v \leq 6.0$. In the $(\overline{\Delta X})$-$(\overline{\Delta R})$ plot, the ferroelectrics occupy the gap between the Chevrel phases and cuprate superconductors. This striking diagrammatic relationship supports ideas concerning a close connection between ferroelectricity and superconductivity, which have arisen in a variety of contexts.[87]

As in the cases of stable quasicrystals and ferroelectrics, the diagrammatic regularities lend themselves to the development of a variety of prediction strategies for new high-T_c superconductors. In Ref. 86 the coordinate restrictions of island C were applied to a set of 332 000 pseudoternary candidate compositions with stoichiometry and chemistry based on $(La,Sr)_2CuO_4$ and $YBa_2Cu_3O_7$. The resulting 234 most favorable combinations are not restricted to oxides, but also include N, the other group-VI elements S, Se, and Te, and the halides F, Cl, Br, and I when combined with suitable cations.

Another search strategy we have pursued is the screening of known ternary-oxide compounds to identify compounds which could act as parent compounds for high-T_c oxide superconductors, in the same way as La_2CuO_4 and $YBa_2Cu_3O_6$. We have examined the Inorganic Crystal Structure Database[8] (ICSD) for ternary oxides located in island C. The resulting list contained about 1500 compounds. To narrow this list, we decided to look for layered compounds with component layers which could serve as templates for CuO_2 or AgO_2 planes. The lattice-constant data included in the ICSD permits the computerized application of the condition that the compounds be tetragonal, i.e., potentially have square planar layers. Forty of the 80 resulting tetragonal compounds have the formula ABO_4 and are not layered, containing linked tetrahedra and octahedra.[72] If we further impose the condition that the basal lattice constant fit within 0.1 Å to that of CuO_2 (3.86 Å) or AgO_2 (4.04 Å), we are left with six compounds of the former type $[La_2(Co,Ni,Cu)O_4$, $Bi_2(Mo,W)O_6$ and $Bi_4Ti_3O_{12}]$ and one of the latter (Ba_2SnO_4). As we see, the six compounds suitable as epitaxial templates for CuO_2 planes have actually all been shown to be the desired antecedents, and no others are known. With Sn in a nominally 4+ state, Ba_2SnO_4 is an unfavorable template for AgO_2 planes. It can independently be argued that it is much harder to oxidize Ag to Ag^{2+} than it is to oxidize Cu to Cu^{2+}. Our point is that even if such oxidation *were* possible, the structural templates for CuO_2 would exist, while those for AgO_2 would not.

Yet another prediction strategy for finding new high-T_c superconductors in island C is based on the previously discussed relationship of this class of materials to high-T_C ferroelectrics. Quite generally, high-T_C ferroelectrics occur already as ABO simple ternaries, while the components of high-T_c superconductive cuprates have the form A-A'-Cu-O. In other words, the metallic character of the superconductors is achieved by adding at least a third metallic element, or fourth element overall. The effect of the extra metallic element on the QSD is to increase $\overline{N}_v$ from 5.0 to 6.3 either directly, with $N_{v,A'} > N_{v,A}$, or indirectly, by inducing an insulator-metal transition which changes the appropriate value of N_v for noble metals to include d electrons; i.e., in insulators, $N_v(\mathrm{Cu})=1$, while in metals, $N_v(\mathrm{Cu})=11$. At the same time, the substitution should be such that $\overline{\Delta R}$ satisfies the rather strict condition for island C, which is contained within the ferroelectric range.

Some specific examples of this relationship can already be found by considering known compounds. The ferroelectric titanates with the highest Curie temperatures are monoclinic $La_2Ti_2O_7$ ($T_C=1770$ K) and tetragonal $Bi_4Ti_3O_{12}$ ($T_C=950$ K). The quasioctahedrally coordinated atom pivotal to the ferroelectric lattice instability is Ti. If we now replace Ti with an appropriate mixture of Cu, to make the material metallic, and an alkaline earth (Ca, Sr, and/or Ba), to yield correct values of $\overline{N}_v$ and $\overline{\Delta R}$, we obtain a high-T_c superconductor, with T_c ranging from 85 to 110 K, depending on details of the layering.[88] Other high-T_C ferroelectric titanates include $Bi_4PbTi_4O_{15}$ ($T_C=840$ K), cubic $PbTiO_3$ ($T_C=760$ K), and a wide variety of pseudoternary perovskites with mixtures of Pb, Bi, and alkaline earths, all with similar or lower T_C's. Much less explored are the tungstates and molydenates, but Bi_2WO_6 is known to have $T_C=1220$ K, and this compound contains the same Bi_2O_2 double-layer structural unit found in $Bi_4Ti_3O_{12}$ and related to that in the high-T_c cuprate superconductors. The development of a systematic procedure, based on these observed relationships, for predicting new high-T_c superconductors from known high-T_C ferroelectrics is currently under investigation.

The prediction strategies described above focus mainly on superconductors in island C. Of course, it is also of interest to apply such strategies to the other islands A and B. The search for new binary representatives in these classes could conceivably be managed with conventional approaches, though even in this case diagrammatic conditions are helpful. What remains to be seen is whether these classes of superconductors contain ternary examples as well. This line of investigation, impossible without the use of the diagram technique, may even push up the limits on T_c in these classes and extend the search for additional liquid-nitrogen-temperature superconductors in radically new directions.

VIII. DISCUSSION

The goal of this paper was to present a self-contained description of the quantum diagram method and to discuss the ways in which it can be used to understand interesting phenomena in materials too complex to be within the scope of normal "chemical intuition," much less to be fully studied from a detailed first-principles approach.

Ideally, the analysis starts with the compilation of a complete database of known compounds exhibiting the phenomenon of interest, the computation of diagrammatic coordinates, and the construction of QSD's and QFD's. Even if the database is small, the observation of localization or other diagrammatic regularities is significant, since the coordinate definitions were previously fixed by analysis of the full intermetallic compound database. This point is crucial, since the databases we consider are too small to support statistically valid analyses if considered independently. At the very least, diagrammatic localization indicates that the property of interest is controlled by chemical factors contained in the diagrammatic coordinate definitions. A comparison with the diagrams for the full database of all known com-

pounds may even suggest structural features or stability information directly resulted to the property of interest. Based on known compounds with this property, the physical interpretations derived from the comparison with the full database of known compounds, and possibly physical ideas from other sources, a list of candidate compositions can be generated and screened for those which satisfy the diagrammatic conditions and thus are especially likely to be successful predictions. Again, however, we emphasize that in our experience so far, the diagrammatic conditions are necessary but not sufficient for occurrence of the property of interest. This is because the subtle energy and entropy factors which ultimately determine, for example, the local stability of a quasicrystalline structure are below the resolution of our analysis. Rather, we identify borderline situations in which small factors would be sufficient and statistically can be expected to be present in some fraction of the total set of predictions.

The application to stable quasicrystallinity is the most exhaustive, illustrating the various principles well. The known stable examples are found to localize very well on the QSD. The larger class of metastable quasicrystals also localize, though less tightly. This localization is in itself remarkable, suggesting that stable quasicrystallinity is controlled by chemical factors contained in the diagrammatic coordinate definitions. The comparison with the full intermetallic QSD further suggests that these factors are closely related to the formation of icosahedral coordination environments in crystalline intermetallic compounds, confirming the physically reasonable idea that a local tendency to icosahedral order is favorable for quasicrystal formation. Even more information about the ternary-alloy systems in which quasicrystals form is available from the QFD. The observed regularities there, combined with the QSD localization, lead to quite restrictive conditions for screening candidate compositions and generating predictions for new quasicrystals.

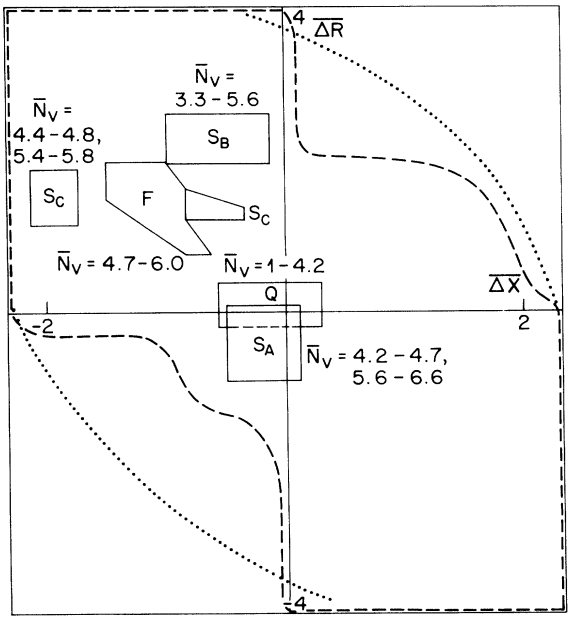

FIG. 14. Schematic overview of the QSD distribution of the stable quasicrystals (Q), high-T_C ferroelectrics (F), and high-T_c superconductors (S_A, S_B, and S_C) relative to each other and to the full database of known intermetallic compounds, indicated by a dotted line. The dashed line shows the distribution of binary compounds, for which complete diagrams are available in Ref. 26. Note the change in scale from previous figures.

For ferroelectrics and superconductors, the presently possible analysis is relatively incomplete. The pronounced localization of high-T_C ferroelectrics and high-T_c superconductors is highly significant. It suggests that local structural and chemical features control these phenomena. The localization of high-T_c superconductors into three distinct islands produces a classification scheme for these materials which transcends structure type. The dependence on T_C or T_c of the localization, and especially of the intimate relationship between ferroelectrics and the superconductors in island C, suggests that conditions on local structure and chemistry are essential features for producing high transition temperatures. Finally, the localization provides an convenient empirical basis for the prediction of new materials. The further development of this analysis, analogous to that for quasicrystals, requires some substantial advances in diagram construction. Most particularly, the ternary- and quaternary-oxide and -halide compounds should be organized via the QSD to identify any features in the coordinate regimes belonging to the ferroelectrics and superconductors which might be associated with these phenomena. In addition, a stability diagram such as QFD, appropriate to oxides, would provide additional useful information. Work on these problems is currently in progress.

This paper is not an exhaustive analysis of the application of diagrams to the physics of quasicrystallinity, ferroelectricity, and superconductivity, but rather a setting forth of the basic principles which guide such applications and a preliminary investigation of these phenomena. Even some familiarity with the background of the diagram technique is enough to understand that the diagrammatic localization and regularities we have described for these materials are by no means incidental or trivial. Moreover, the diagrams provide a powerful tool for visualizing the trends and relationships in enormous amounts of data in a wide variety of systems, permitting us, for example, to summarize in a single figure (Fig. 14) the relationship of stable quasicrystals, high-T_C ferroelectrics, and high-T_c superconductors to each other and to the full database of known compounds. Such analyses can in the future be straightforwardly applied to other phenomena, such as magnetism, for which local crystal structure, chemistry, and stability are expected to play an important role. However, the use of diagrams as a tool in understanding the physics of these phenomena and in predicting new materials is still in the early stages of development, with many exciting speculations suggesting new lines for further exploration.

APPENDIX: DEFINITIONS OF ATOMIC PARAMETER SCALES

In the statistical approach to diagram construction, it is required that the diagrammatic coordinates be simple

functions of parameters assigned to atoms. Moreover, these parameters are expected to be definable on an equal footing for all atoms in the periodic table (except noble gases) and be uniquely defined by the atom independent of the crystal environment. This high level of transferability is an extremely stringent demand, and to satisfy it inevitably involves a compromise on the absolute accuracy of the description. One might, however, worry that there is insufficient room for approximations, since the energy differences between competing structures for a given composition are generally very small. Indeed, in first-principles calculations it can be difficult to get the hierarchy right and the final determining effects can seem very subtle. How, then, is it possible for such a simple structural analysis scheme to work so well?

To understand the successes of this method, it is vital to examine the behavior of the atomic parameter scales and their physical interpretation. In doing this it is useful to take advantage of the two-step nature of the statistical derivation. First, we look at the trends exhibited by atomic parameter scales which were identified as relevant to the determination of crystal structure. Out of five classes $A-E$, class A_1 (a subtype of class A), D, and E are singled out. Representative of class A_1 are the pseudopotential core radii.[6] The trend in this class is to decrease fairly smoothly across each row of the periodic table and increase down each column. Incidentally, crystallographic definitions of ionic, metallic, and covalent radii are in the closely related, but different, classes A_2 and A_3. Class D contains, among many other properties, all definitions of electronegativity. The trend in class D is to increase up to the beginning of the transition metals, then more or less decrease across the transition metals, making a small jump down to the noble metals, and then increasing again. Class E, the simplest example of which is the valence electron number, increases smoothly from group IA to the end of the transition metals, then jumps down, and increases again to group VIIA. The trends in D and E are in fact similar for simple metals and are distinguished primarily by opposite slopes in the transition-metal region.

The second step in the process is to identify the optimal definitions in each class. For compounds far away from structural boundaries, this level of refinement is relatively unimportant, while it is crucial in sorting out compounds near boundaries that separate two different structures. Parameter scales with qualitatively the same general trends can lead to very different assessments of "chemical similarity" based on the numerical differences between atoms. The most successful elemental scales are the pseudopotential core radii (A_1), electronegativity defined according to the Martynov-Batsanov prescription (D), and the valence-electron number (E).

It is very significant that the most successful coordinates are descriptive of properties of the valence electrons, which is what would be expected, since they dominate bonding properties. It is also interesting that out of the great variety of properties examined, the statistical analysis should pick out the ones which have the most obvious relationship to bonding and are *derived from explicitly quantum-mechanical prescriptions rather than empirically*. Examination of the precise definitions of these scales should give information about exactly what is and what is not included in this description.

The pseudopotential core radii are the optimal elemental coordinates in class A_1. They give a measure of size which is directly related to the size of the core. In contrast to crystallographic radii, which depend on valence and coordination, the pseudopotential core radii have the advantage of being defined for an atom independent of its environment. On the other hand, superficially one might think that crystallographic radii would be significantly more effective in providing structural information, but statistical analysis of AB CsCl vs NaCl structures show that this is not the case.[9]

The sense in which structural information is contained in the pseudopotential core radii can be better understood by closer examination of their definition. Pseudopotentials are constructed by making a linear combination of core wave functions with the valence wave function of the same l to obtain a nodeless pseudo-wavefunction. Inversion of the Schrödinger equation yields nonlocal (l-dependent) hard-core pseudopotentials which are strongly repulsive at small r, becoming attractive for values of r outside the core radius. The value of r at which the pseudopotential crosses zero defines the core radius for that value of l. Inclusion of the centrifugal potential means that even in the case where there are no core electrons of the same l the potential has this same hard-core shape and the pseudopotential core radius can be defined. The use of screened pseudopotentials for this definition has a number of advantages. First, the screened pseudopotential is directly related to the shape of the corresponding wave function. Also, the radius for a particular l does not depend on the assignment of shells of electrons of other angular momentum as core or valence. This is particularly important for noble metals in which it may be appropriate to assign the d electrons either as core or valence, while the values of r_s and r_p would be unaffected.

From the definition of radius through the hard-core pseudopotential, its role in structural properties can be deduced. First, the pseudopotential core radius certainly contains an essential part of the information from which bond lengths and other essential aspects of crystalline geometry are derived. These radii, combined with the other diagrammatic coordinates, yield a picture of the electronic charge distribution from which can be extracted the crystallographic radii so useful in the analysis of specific structures. Also, it is interesting to note that even for the transition- and noble-metal compounds, the core radii r_s and r_p are still adequate for the description of structure, without any inclusion of r_d. This is because the d electrons are spatially highly localized, with typically $r_d < r_s, r_p$ by at least a factor of 2, and are not involved in determining bond lengths.

Class D contains a large number of different atomic properties. The property picked out by the statistical analysis as being most effective in structural separation is the electronegativity defined according to the Martynov-Batsanov scale.[10] The effectiveness of the electronegativity is not very surprising, since the concept itself was

designed to describe bonding—more specifically, that aspect of bonding associated with the relative ability of an atom in a molecule or solid to attract valence electrons. The construction of a quantitative scale which can be used to measure this attractive ability has proven to be less straightforward, however, and a variety of different electronegativity scales exist which even vary according to the units in which electronegativity is measured.

As in the case of radii, for electronegativity there is a marked distinction between "crystallographic" definitions, which are based on a single-scale relationship between some experimentally measured solid-state property and electronegativity, and "diagrammatic" definitions, which optimize the effectiveness of the electronegativity scale for structural separations when used in combination with other scales. The best example of the crystallographic type of scale, the Pauling scale, is also the most familiar. It is based on extensive heat of formation data in binary compounds and the assumption of additivity of bond energies. In contrast, the optimal diagrammatic scale, Martynov-Batsanov electronegativity, is based solely on atomic ionization potentials with no empirical input of solid-state properties. More precisely, the Martynov-Batsanov electronegativity X_{MB} is defined as

$$X \equiv 0.39\sqrt{\bar{E}} \ ,$$

with

$$\bar{E} = \frac{1}{m} \sum_{i=1}^{m} I_i \ .$$

I_i are atomic ionization potentials, and $i = 1, 2, \ldots, m$ indexes the valence electrons. Thus $\bar{E}$ is a measure of the average energy of the valence electrons. The square root and constant 0.39 are chosen to maximize numerical similarity with the Pauling scale for first-period elements.

The Martynov-Batsanov electronegativity values are listed in Fig. 1. It is important to note that the definition as originally stated depends on chemical valence, thus giving more than one value for certain atoms. In each case we have chosen the highest valence value. For nearly all atoms, this coincides with our definition of the number of valence electrons, discussed further below. The exceptions are those near the end of the transition series: Cr, Mn, and group-VIIIA elements. This discrepancy is responsible for the rather jagged behavior across the transition-metal series. It is not clear at present whether this feature of the overall trend is more or less favorable for structural separation than a fully consistent version, smoothly increasing through the transition metals, would be.

The reason that the electronegativity plays such an important role in structural determination is that it helps to determine the charge distribution by measuring the competing attraction of different atoms for the available valence electrons. Larger electronegativity differences imply that the system is more ionic and that crystal structures characteristic of ionic bonding are favored. Smaller electronegativity differences reduce the tendency for electrons to become associated with a particular atom, thus favoring metallic or covalent structure types. The association of electrons with a particular atom can also affect the orbital character of the states.

In class E the optimal character of the valence-electron number is not surprising, as it is clearly a key factor in any description of chemical bonding. The precise definition of the valence-electron number we use needs some comment. In particular, it is not exactly the same as the atomic valence, differing from it for atoms which have more than one valence. For transition metals we count the total number of electrons in the outer s, p, and d shells. For noble metals it turns out to be very worthwhile to relax the strict rule of one parameter per atom in order to obtain a correct description of the behavior of these elements. For studying metallic compounds, for the Cu and Zn columns, we use $N_v = 11$ and 12, while for studying insulators, the outermost d electrons are included in the core and $N_v = 1$ or 2. Pending further investigation, we tentatively assign $N_v = 3$ to the lanthanides and actinides.

Aside from the more obvious significance of the number of valence electrons, there are two cases in which the total number of valence electrons plays a decisive role in determining structure. The first is for certain alloys of simple metals, where the Hume-Rothery rules describe sudden changes in relative stability of different structures at special values of the electron-atom ratio (related to $\sum N_v$). Second, as we shall discuss further in the next paragraph, the total valence-electron number turns out to be crucial for the correct inclusion in the diagrams of structure types stabilized by covalent bonding.

To conclude, let us consider the total picture of a solid which can be constructed using the information in these parameters. A collection of ion cores acts on a given total number of valence electrons. If the electronegativity difference between component atoms is large, electrons will primarily be associated with cores to form ions. For small electronegativity differences, the bonding will have a more metallic or covalent character. Effective radii are determined by a combination of the pseudopotential radii and the electron distribution resulting from electronegativity differences. The ionic, metallic, or covalent nature of the bonding and the effective radii together are the essential ingredients in determining the structural geometry. The main difficulty is in distinguishing between the metallic and covalent cases. Since the information needed to describe directional hybridized bonding effects is not included as a diagrammatic coordinate, it may seem surprising that obviously covalent structures such as zinc blende are correctly separated. In fact, examination of the AB diagrams shows that "covalent" structures are highly localized in $\sum N_v$, yielding thin "pancake" islands which can be assigned to the correct structure types without producing a significant number of violations. This behavior is best illustrated by the zinc-blende structure, with $\sum N_v = 8$, for which the covalent character of the bonding is well established. In general,

an island with this characteristic shape could be inferred to be stabilized by covalent forces. Finally, while more detailed aspects of the structure, such as small Jahn-Teller distortions, require knowledge of directional bonding and other exceptional factors beyond the scope of the diagrammatic coordinates, the general structure type, and thus the validity of the diagrammatic description, is unaffected by these considerations.

ACKNOWLEDGMENTS

We are grateful to John Merrall for his assistance in searching the ICSD for ternary superconductive archetypes and to A. R. Kortan for invaluable discussions. One of us (K.M.R.) acknowledges support by the Clare Boothe Luce Fund, NSF Grant No. DMR-9057442, and ONR Grant No. N00014-91-J-1247.

[1]J. C. Phillips, in *Treatise on Solid State Chemistry,* edited by N. B. Hannay (Plenum, New York, 1976), Vol. 1, p. 1.
[2]J. C. Phillips, Helv. Phys. Acta **58**, 209 (1985).
[3]J. C. Phillips, in *Electronic Materials: A New Era of Materials Science,* edited by J. R. Chelikowsky and A. Franciosi (Springer, New York, in press).
[4]W. B. Pearson, *The Crystal Chemistry and Physics of Metals and Alloys* (Wiley, New York, 1972).
[5]J. C. Phillips and J. A. Van Vechten, Phys. Rev. B **2**, 2147 (1970); J. C. Phillips, Rev. Mod. Phys. **42**, 317 (1970).
[6]A. Zunger and M. L. Cohen, Phys. Rev. B **20**, 4082 (1979); A. Zunger, in *Structure and Bonding in Crystals,* edited by M. O'Keefe and A. Navrotsky (Academic, New York, 1981).
[7]P. Villars and L. D. Calvert, *Pearson's Handbook of Crystallographic Data for Intermetallic Phases* (American Society of Metals, Metals Park, OH, 1985).
[8]G. Bergerhoff, R. Hundt, R. Sievers, and I. D. Brown, J. Chem. Inf. **23**, 66 (1983).
[9]P. Villars, J. Less-Common Met. **92**, 215 (1983).
[10]A. J. Martynov and S. S. Batsanov, Russ. J. Inorg. Chem. **25**, 1737 (1980).
[11]S. B. Zhang, M. L. Cohen, and J. C. Phillips, Phys. Rev. B **36**, 5861 (1987); **38**, 12 085 (1988).
[12]G. Simons and A. N. Bloch, Phys. Rev. B **7**, 2754 (1973); J. R. Chelikowsky and J. C. Phillips, *ibid.* **17**, 2453 (1978).
[13]D. G. Pettifor, J. Phys. C **19**, 285 (1986).
[14]J. C. Phillips, Phys. Rev. B **37**, 2483 (1988).
[15]P. Villars, J. Less-Common Met. **99**, 33 (1984).
[16]P. Villars, J. Less-Common Met. **102**, 199 (1984).
[17]P. Villars (unpublished).
[18]The example of CuF is discussed in J. R. Chelikowsky and J. C. Phillips, Phys. Rev. B **17**, 2453 (1978).
[19]B. K. Godwal, V. Vijaykumar, S. K. Sikka, and R. Chidambaram, J. Phys. F **16**, 1415 (1986).
[20]F. Merlo and M. L. Fornasini, J. Less-Common Met. **119**, 45 (1986).
[21]W. Andreoni, G. Galli, and M. Tosi, Phys. Rev. Lett. **55**, 1734 (1985).
[22]J. R. Chelikowsky, Phys. Rev. Lett. **58**, 714 (1987).
[23]P. Villars and F. Hulliger, J. Less-Common Met. **132**, 289 (1987).
[24]P. I. Kripyakevich, Zh. Strukt. Khim. **4**, 117 (1963); **4**, 282 (1963) [J. Struct. Chem. **4** (1963)].
[25]G. O. Brunner and D. Schwarzenbach, Z. Kristallogr. **133**, 127 (1971).
[26]P. Villars, K. Mathis, and F. Hulliger, in *The Structures of Binary Compounds,* edited by F. R. de Boer and D. G. Pettifor (North-Holland, Amsterdam, 1989), Vol. 2, p. 1.
[27]P. Villars, J. Less-Common Met. **109**, 93 (1985).
[28]A. R. Miedema, J. Less-Common Met. **46**, 67 (1976); A. Zunger, Phys. Rev. B **22**, 5839 (1980).
[29]P. Villars, J. Less-Common Met. **119**, 175 (1986).
[30]R. J. Schaefer and L. A. Bendersky, in *Introduction to Quasicrystals,* edited by M. V. Jarić, *Aperiodicity and Order,* Vol. 1 (Academic, New York, 1988), p. 111.
[31]R. W. Cahn, Nature **341**, 183 (1989).
[32]D. Shechtman, I. Blech, D. Gratias, and J. W. Cahn, Phys. Rev. Lett. **53**, 1951 (1984).
[33]P. A. Bancel and P. A. Heiney, Phys. Rev. B **33**, 7917 (1986).
[34]R. A. Dunlap and K. Dini, Can. J. Phys. **63**, 1267 (1985).
[35]P. Ramachandrarao and G. V. S. Sastry, Pramana **24**, L225 (1985).
[36]G. V. S. Sastry, P. Ramachandrarao, and T. R. Anantharaman, Scr. Metall. **20**, 191 (1986).
[37]H. S. Chen, J. C. Phillips, P. Villars, A. R. Kortan, and A. Inoue, Phys. Rev. B **35**, 9326 (1987).
[38]Z. Zhang, H. Q. Ye, and K. H. Kuo, Philos. Mag. A **52**, L49 (1985); Z. Zhang and K. H. Kuo, Philos. Mag. B **54**, L83 (1986).
[39]C. Dong, Z. K. Hei, L. B. Wang, Q. H. Song, Y. K. Wu, and K. H. Kuo, Scr. Metall. **20**, 1155 (1986).
[40]K. H. Kuo, C. Dong, D. S. Zhou, Y. X. Guo, Z. K. Hei, and D. X. Li, Scr. Metall. **20**, 1695 (1986).
[41]K. H. Kuo, D. S. Zhou, and D. X. Li, Philos. Mag. Lett. **55**, 33 (1987).
[42]L. A. Bendersky and F. S. Biancaniello, Scr. Metall. **21**, 531 (1986).
[43]P. A. Bancel, P. A. Heiney, P. W. Stephens, A. I. Goldman, and P. M. Horn, Phys. Rev. Lett. **54**, 2422 (1985).
[44]D. Levine and P. J. Steinhardt, Phys. Rev. Lett. **53**, 2477 (1984).
[45]V. Elser, Phys. Rev. B **32**, 4892 (1985).
[46]P. W. Stephens and A. I. Goldman, Phys. Rev. Lett. **56**, 1168 (1986); P. W. Stephens, in *Extended Icosahedral Structures,* edited by M. V. Jarić and D. Gratias, *Aperiodicity and Order,* Vol. 3 (Academic, New York, 1989), p. 37.
[47]P. M. Horn, W. Malzfeldt, D. P. DiVincenzo, J. Toner, and R. Gambino, Phys. Rev. Lett. **57**, 1444 (1986).
[48]P. Sainfort and B. Dubost, J. Phys. (Paris) Colloq. **47**, C3-321 (1986); W. A. Cassada, G. J. Shiflet, and S. J. Poon, Phys. Rev. Lett. **56**, 2276 (1986).
[49]W. Ohashi and F. Spaepen, Nature **230**, 555 (1987).
[50]A. P. Tsai, A. Inoue, and T. Masumoto, Jpn. J. Appl. Phys. **26**, L1505 (1987); K. Hiraga, B. P. Zhang, M. Hirabayashi, A. Inoue, and T. Masumoto, *ibid.* **27**, L951 (1988); A. P. Tsai, A. Inoue, and T. Masumoto, *ibid.* **27**, L1587 (1988).
[51]A. P. Tsai, A. Inoue, and T. Masumoto, Mater. Trans. JIM **30**, 463 (1989).
[52]A. P. Tsai, A. Inoue, Y. Yokoyama, and T. Masumoto, Mater. Trans. JIM **31**, 98 (1990).
[53]A. R. Kortan, H. S. Chen, and F. A. Thiel, Bull. Am. Phys. Soc. **34**, 408 (1989); C. A. Guryan, A. I. Goldman, P. W. Stephens, K. Hiraga, A. P. Tsai, A. Inoue, and T. Masumoto, Phys. Rev. Lett. **62**, 2409 (1989).

[54]P. Villars, J. C. Phillips, and H. S. Chen, Phys. Rev. Lett. **57**, 3085 (1986).

[55]K. M. Rabe, A. R. Kortan, J. C. Phillips, and P. Villars, Phys. Rev. B **43**, 6280 (1991).

[56]J. Tartas and E. J. Knystautas, J. Mater. Res. **6**, 1219 (1991).

[57]K. J. Strandburg, Phys. Rev. B **40**, 6071 (1989), and references cited therein.

[58]K. J. Strandburg, L-H Tang, and M. V. Jarić, Phys. Rev. Lett. **63**, 314 (1989); M. Widom, D. P. Deng, and C. L. Henley, *ibid.* **63**, 310 (1989). For a two-dimensional model, these authors found a configurational entropy contribution to the free energy of the same order of magnitude as the energy differences due to farther-neighbor van der Waals interactions. In real intermetallic systems, there are additional contributions to effective long-range interatomic interactions which typically make the structural energy differences much larger.

[59]D. P. Shoemaker and C. B. Shoemaker, in *Introduction to Quasicrystals,* edited by M. V. Jarić, *Aperiodicity and Order,* Vol. 1 (Academic, New York, 1988), p. 1.

[60]F. C. Frank and J. S. Kasper, Acta Crystallogr. **11**, 184 (1958); **12**, 483 (1959); W. B. Pearson, *The Crystal Chemistry of Metals and Alloys* (Wiley, New York, 1972).

[61]V. Elser and C. L. Henley, Phys. Rev. Lett. **55**, 2883 (1985); P. Guyot and M. Audier, Philos. Mag. B **52**, L15 (1985).

[62]M. Widom, K. J. Strandburg, and R. H. Swendsen, Phys. Rev. Lett. **58**, 706 (1987); S. Narasimhan and M. V. Jarić, *ibid.* **62**, 454 (1989).

[63]M. G. Bown and P. J. Brown, Acta Crystallogr. **9**, 911 (1956).

[64]J. C. Phillips and K. M. Rabe, Phys. Rev. Lett. **66**, 923 (1991).

[65]Y. Yokoyama, A. P. Tsai, A. Inoue, T. Masumoto, and H. S. Chen (unpublished).

[66]R. B. Phillips and A. E. Carlsson (private communication).

[67]J. Friedel, Helv. Phys. Acta A **61**, 538 (1988).

[68]N. F. Mott and H. Jones, *The Theory of the Properties of Metals and Alloys* (Clarendon, Oxford, 1936).

[69]L. A. Bendersky and M. J. Kaufman, Philos. Mag. B **53**, L75 (1986); A. Inoue, K. Nakano, T. Masumoto, and H. S. Chen, Mater. Trans. JIM **30**, 200 (1989).

[70]N. K. Mukhopadhyay, G. N. Subbanna, S. Ranganathan, and K. Chattopadyay, Scr. Metall. **20**, 525 (1986).

[71]A good introduction to ferroelectricity is G. Burns, *Solid State Physics* (Academic, New York, 1985), Chap. 14.

[72]O. Muller and R. Roy, *The Major Ternary Structural Families* (Springer-Verlag, New York, 1974).

[73]E. A. Wood, Acta Crystallogr. **4**, 353 (1951).

[74]P. Villars, J. C. Phillips, K. M. Rabe, and I. D. Brown, Ferroelectrics (to be published).

[75]T. Mitsui *et al.*, in *Ferro- and Antiferroelectric Substances,* edited by K.-H. Hellwege and A. M. Hellwege, Landolt-Börnstein, Vol. 3 (Springer, New York, 1969), pp. 16–35.

[76]T. Mitsui *et al.*, in *Ferro- and Antiferroelectric Substances,* edited by K.-H. Hellwege and A. M. Hellwege, Landolt-Börnstein, Vol. 9 (Springer, New York, 1975), pp. S14–S52.

[77]T. Mitsui *et al.*, in *Ferroelectrics: Oxides,* edited by K.-H. Hellwege and A. M. Hellwege, Landolt-Börnstein, Vol. 16a (Springer, New York, 1981), pp. 21–42.

[78]M. E. Lines and A. M. Glass, *Principles and Applications of Ferroelectrics and Related Materials* (Clarendon, Oxford, 1977), pp. 163 and 620–632.

[79]F. Jona and G. Shirane, *Ferroelectric Crystals* (Pergamon, Oxford, 1962), pp. 217, 253, and 276.

[80]R. Blinc and B. Zeks, *Soft Modes in Ferroelectrics and Antiferroelectrics* (North-Holland, Amsterdam, 1974), pp. 282–297.

[81]V. M. Gurevich, *Electric Conductivity of Ferroelectrics* (Israel Program of Scientific Translation, Jerusalem, 1971), pp. 2–11.

[82]B. T. Matthias, Phys. Today **24**(8), 23 (1971).

[83]S. C. Abrahams and E. T. Keve, Ferroelectrics **2**, 129 (1971).

[84]S. C. Abrahams, Ferroelectrics **104**, 37 (1990), and references cited therein.

[85]J. C. Phillips, *Physics of High-T_c Superconductors* (Academic, Boston, 1989).

[86]P. Villars and J. C. Phillips, Phys. Rev. B **37**, 2345 (1988).

[87]B. T. Matthias, Mater. Res. Bull. **5**, 665 (1970). Many of the ideas in this paper are the result of stimulating discussions in the past with Matthias, who always suspected that high-T_C ferroelectrics and high-T_c superconductors were similar in some ways that were not specifiable at that time.

[88]M. A. Subramanian, C. C. Torardi, J. C. Calabrese, J. Gopalakrishnan, K. J. Morrissey, T. R. Askew, R. B. Flippen, U. Chowdhry, and A. W. Sleight, Science **239**, 1015 (1988).